USGS
science for a changing world

NATIONAL PARK SERVICE

FRIENDS OF HERRING RIVER

Prepared in cooperation with the National Park Service and the Friends of Herring River

Assessment of Prerestoration Water Quality in the Herring River To Support Adaptive Management at the Cape Cod National Seashore

Scientific Investigations Report 2023–5120

U.S. Department of the Interior
U.S. Geological Survey

Caption. U.S. Geological Survey (USGS) hydrologist installing equipment at the Herring River gage at the dike on Chequessett Neck Road (station 011058798) USGS streamgage near Wellfleet, Mass., on Cape Cod used for data collection for the assessment of prerestoration water quality in the Herring River; photograph by Thomas G. Huntington, USGS.

Assessment of Prerestoration Water Quality in the Herring River To Support Adaptive Management at the Cape Cod National Seashore

By Thomas G. Huntington

Prepared in cooperation with the National Park Service and the Friends of Herring River

Scientific Investigations Report 2023–5120

U.S. Department of the Interior
U.S. Geological Survey

U.S. Geological Survey, Reston, Virginia: 2023

Suggested citation:
Huntington, T.G., 2023, Assessment of prerestoration water quality in the Herring River to support adaptive management at the Cape Cod National Seashore: U.S. Geological Survey Scientific Investigations Report 2023–5120, 51 p., https://doi.org/10.3133/sir20235120.

Associated data for this publication:
Huntington, T.G., 2023, Data supporting analysis of relations between nutrient concentrations in the Herring River on the ebb tide, near Wellfleet, Massachusetts, and environmental conditions, 2015–2022: U.S. Geological Survey data release, https://doi.org/10.5066/P9ZU5YHW.

ISSN 2328-0328 (online)

Acknowledgments

This project was supported by funding from the U.S. Geological Survey (USGS) and National Park Service (NPS) cooperative Natural Resources Preservation Program (NRPP) program and the Friends of Herring River. The author is grateful for support received from several people who contributed to the successful completion of this study. Timothy Smith at the Cape Cod National Seashore of the NPS provided technical and logistical support and facilitated sample collection and handling by Kaitlyn Button and Eliza Fitzgerald of the NPS. Cheryl Wiles of the U.S. Forest Service provided analysis of dissolved organic carbon.

The author is grateful to the following USGS personnel who contributed to the study and report. Craig Brown helped with quality assurance analysis, data input into the National Water Information System, and use of gridMET and the Thornthwaite water balance model. Kirk Smith developed software that were used to identify the times for sample collection. Jason Sorenson retrofitted sampling and level-sensor equipment. Ben Rau and Leslie DeSimone helped design the water quality sampling and processing protocols and data review and validation. Mark Nardi and Jason Sorenson provided peer reviews. Janet Barclay provided the R scripts that produced the boxplots included in the report.

Contents

Figures

Tables

Conversion Factors

International System of Units to U.S. customary units

Multiply	By	To obtain
millimeter (mm)	0.03937	inch (in.)
meter (m)	3.281	foot (ft)
kilometer (km)	0.6214	mile (mi)
square meter (m^2)	0.0002471	acre
hectare (ha)	2.471	acre
square kilometer (km^2)	247.1	acre
liter (L)	1.057	quart (qt)

Temperature in degrees Celsius (°C) may be converted to degrees Fahrenheit (°F) as follows:

$$°F = (1.8 \times °C) + 32.$$

Datums

Vertical coordinate information is referenced to the North American Vertical Datum of 1988 (NAVD 88).

Horizontal coordinate information is referenced to the North American Datum of 1983 (NAD 83).

Altitude, as used in this report, refers to distance above the vertical datum.

Supplemental Information

Specific conductance is given in microsiemens per centimeter at 25 degrees Celsius (µS/cm at 25 °C).

Concentrations of chemical constituents in water are given in either milligrams per liter (mg/L) or micrograms per liter (µg/L).

Solar radiation (irradiance), measured as the power received from the Sun per surface area, is measured in watts per square meter (W/m^2).

Abbreviations

DOC	dissolved organic carbon
NADP	National Atmospheric Deposition Program
NH_4	ammonium
NO_2	nitrite
NO_3	nitrate
NOAA	National Oceanographic and Atmospheric Administration
NPS	National Park Service
NWIS	National Water Information System
RPD	relative percent difference
SiO_2	silica
TDN	total dissolved nitrogen
TDP	total dissolved phosphorus
TN	total nitrogen
TP	total phosphorus
USGS	U.S. Geological Survey

Assessment of Prerestoration Water Quality in the Herring River To Support Adaptive Management at the Cape Cod National Seashore

By Thomas G. Huntington

Abstract

In 2020 and 2021, the U.S. Geological Survey, Cape Cod National Seashore of the National Park Service, and Friends of Herring River cooperated to assess nutrient and suspended sediment concentrations across the ocean-estuary boundary at a dike on the Herring River on Chequessett Neck Road in Wellfleet, Massachusetts, that has restricted saltwater inputs by regulating water inflow through three culverts or sluiceways into the watershed for more than 100 years. The dike is slated to be removed, and the purpose of this project was to characterize natural variability of nutrient and suspended sediment concentration during flood tide and ebb tide conditions at the dike based on seasonal and environmental variables. This baseline can be used to assess if removal of the dike is likely to result in measurable changes in water quality.

Data from the current [2023] study were aggregated with previously published data from November 2015 through September 2018 to provide a long-term record. Samples for the current [2023] study were collected from flood and following ebb tides approximately twice per month from June 2020 through December 2021 at fixed time intervals after the beginning of the tides. Samples were analyzed for nitrate plus nitrite, ammonium, total dissolved nitrogen, total nitrogen, orthophosphate, total dissolved phosphorus, total phosphorus, silica, dissolved organic carbon, and suspended sediment. Constituent concentrations generally were lower using fixed time sampling than in previous studies that used flow-weighted composite sampling, except for nitrate plus nitrite and orthophosphate. Concentrations of nitrate plus nitrite, ammonium, total nitrogen, total dissolved nitrogen, silica, and dissolved organic nitrogen generally were higher on the ebb tide than on the flood tide. By contrast, concentrations of orthophosphate, total phosphorus, and total dissolved phosphorus were generally similar between flood and ebb tides.

Most nutrient concentrations except silica and ammonium varied seasonally on flood and ebb tides. Phosphorus species, total nitrogen, and dissolved organic carbon concentrations generally peaked in mid- to late summer and were lowest in winter. For nitrate, the reverse was true. Nutrient concentrations generally were higher on the ebb tide than on the flood tide except for total dissolved phosphorus and total phosphorus where differences between flood and ebb tide depended on season. Constituent concentrations were similar between spring, neap, and midamplitude tides on both the flood and ebb tides.

Nitrate, ammonium, total nitrogen, and silica concentrations were positively correlated with precipitation and runoff. Orthophosphate, total dissolved phosphorus, total phosphorus, and dissolved organic carbon were positively correlated with surface air temperature, downwelling shortwave radiation, and ocean water temperature. Nitrate, ammonium, and silica concentration were negatively correlated with surface air temperature and ocean water temperature. Orthophosphate and total dissolved phosphorus were negatively correlated with runoff. Nitrate plus nitrite, ammonium, and silica concentrations were negatively correlated with downwelling shortwave radiation.

Introduction

The Herring River estuary in Wellfleet and Truro, Massachusetts, has been diked off from the ocean for more than 100 years; this has led to a degradation of habitats with severe ecological consequences both upstream and downstream from the dike (Soukup and Portnoy, 1986; Portnoy and Giblin, 1997a, b; Portnoy and Allen, 2006; National Park Service and others, 2016). Habitat degradation in surface waters has included depletion of dissolved oxygen, increased acidity and aluminum, methane emissions, and increases in fecal coliform concentrations. The National Park Service (NPS) is planning to remove the existing dike structure and replace it with a new structure that would include several culverts and the capacity to adjust tidal inputs (National Park Service and others, 2016). The planned restoration of tidal flushing is expected to result in improvements in coastal habitat, ecosystem services, and water quality from increased tidal exchange. Restoration could also result in increased nutrient fluxes, sulfide accumulation in soils, and short-term mobilization and transport of fine-grained sediment. Changes in water

quality during and following restoration could have effects on shellfish aquaculture in Wellfleet Harbor (National Park Service and others, 2016).

A previous study conducted at the same location showed substantial temporal variation in nutrient and sediment concentrations (Huntington and others, 2021). Therefore, it is important to monitor nutrient concentrations over as broad a range of hydroclimatic conditions as possible to encompass the full range of natural variability under the current [2023] dike configuration. Also, the tidal exchange of dissolved and particulate organic carbon remains poorly understood, leading to a data gap in the effects of restoration of tidal exchange on the Herring River carbon budget. To resolve these knowledge deficits and provide data that may be used to model and predict change prompted by restoration, robust baseline information is needed on aquatic concentrations of nutrients, sediment, and dissolved and particulate organic carbon. This project addresses these needs by providing a comprehensive dataset on the tidal-cycle concentrations of these constituents that could be used in future studies to estimate their aquatic fluxes for the baseline pre-restoration period.

The National Park Service (NPS) is planning to remove the existing dike structure and replace it with a new structure that would include several culverts and the capacity to adjust tidal inputs (National Park Service and others, 2016). To help park resource managers determine if post-restoration conditions fall outside the range of pre-restoration variation, the NPS has developed an adaptive management plan to guide decisions during the restoration (National Park Service and others, 2016; Town of Wellfleet, 2019). The adaptive management plan is a phased reintroduction of tidal inputs into the estuary and permits adjustment of flows if undesirable changes in water quality are observed. The adaptive management plan includes monitoring nutrient and suspended sediment concentration during restoration and comparisons of these measurements with the pre-restoration baseline to support decisions about how best to manage tidal inputs. Information is needed to place the baseline water quality data in the context of the previously published data and describe the variability in water quality in relation to season, tidal, and hydroclimatic conditions.

Background Information

Historically, the Herring River estuary and flood plain was the largest tidal river and estuary complex on Outer Cape Cod and included about 6 square kilometers (km^2; 600 hectares [ha]) of salt marsh, intertidal flats, and open-water habitats (National Park Service and others, 2016). These habitats are critically important for native vegetation and their inherent ecological functions as nurseries for marine animals; nesting and feeding areas for a variety of mammal, bird, amphibian, and fish species; and migratory pathways for anadromous species. Restoration of this resource would enhance its value for wildlife and recreational opportunities, including canoeing, kayaking, fishing, and viewing wildlife in restored wetlands and open-water habitats. Salt marsh restoration, defined as movement towards goals in vegetation, fish, and bird assemblages by restoring previously restricted tidal inputs, has been documented in New England (Warren and others, 2002; Chaffee and others, 2012; Roman and Burdick, 2012).

The town of Wellfleet is preparing to restore the Herring River estuary, which is within the Cape Cod National Seashore and managed by the NPS and has been diked off from the ocean for more than 100 years. The restoration plan consists of replacing the existing dike with a bridge and control gates to restore tidal flushing to large parts of the former salt marsh. Restoration is expected to improve water and soil quality, increase river herring and shellfish habitat, minimize the spread of invasive plant species, and provide improved recreational opportunities, among other benefits (Portnoy, 1999; Portnoy and Allen, 2006; National Park Service and others, 2016). To monitor biogeochemical and hydrologic changes in response to increased tidal exchange, flows would be increased incrementally during an adaptive management phase using adjustable gates at the new control structure on Chequessett Neck Road (Town of Wellfleet, 2019). The project is a partnership between the Cape Cod National Seashore and the Town of Wellfleet.

Diking and subsequent tidal restriction has resulted in loss of substantial areas of (tidal) salt and brackish marsh and increases in wet shrubland, wet and dry deciduous forests, and freshwater marsh in the Herring River Watershed (National Park Service and others, 2016). Habitat degradation in surface waters includes depletion of dissolved oxygen, increases in acidity and aluminum concentrations (that can be toxic to sensitive aquatic biota), and increases in fecal coliform concentrations (Portnoy and Allen, 2006). Diking has profoundly altered the hydrology and chemistry of the marsh upstream of the dike (Soukup and Pornoy, 1986). Portnoy and Giblin (1997a, b) described two distinctly different altered marsh environments after the installation of a dike: one system as diked drained, and a second system as diked and seasonally flooded.

In the diked drained systems, dewatering has resulted in air penetration into previously anoxic sediments that has led to oxidation of pyrite and generation of acidity and release of toxic aluminum concentrations (Portnoy and Giblin, 1997a). Aerobic conditions in the organic sediments facilitated rapid decomposition compared with conditions before installation of a dike. Rapid decomposition has resulted in substantial subsidence of the marsh surface (of 1 meter [m] or more, relative to contemporary sea level) in some places. The marsh surface elevation must increase at a rate greater than or equal to the rate of sea-level rise or risk inundation and loss of vegetation and ecosystem services. The dynamics of marsh elevation change depend on various processes, including sediment transport and deposition on marsh surfaces and the growth of salt marsh vegetation. Diking and drainage has effectively prevented sediment from reaching many areas of the Herring River flood plain, and restoration is expected to increase sediment deposition on marsh surfaces (National Park Service and others, 2016).

Concentrations of nitrogen and phosphorus in the sediments of Herring River have remained high in recent years (National Park Service and others, 2016). Potential sources of nutrient inputs to the watershed include agriculture, fertilized lawns, a golf course, a nearby landfill, septic systems, animal waste, and atmospheric deposition. The inputs have not been quantified. The lack of tidal flushing has allowed nutrients to accumulate in the Herring River watershed. In the diked drained sediments, ammonium (NH_4) has accumulated on sediment ion exchange surfaces, and orthophosphate (PO_4^{3-}) has accumulated on iron oxides. Column experiments have indicated that restoration of saltwater tidal flushing in these sediments will likely result in mobilization and release of NH_4, PO_4, and iron (Portnoy and Giblin, 1997a). The Wellfleet Harbor aquaculture industry brings in more than 5 million dollars each year. A major nutrient release, even if short-lived, could result in eutrophication leading to hypoxia and adversely affect the industry. This specific concern is one of the major reasons that the restoration plan includes a phased or incremental reintroduction of saltwater to allow for adaptive management (National Park Service and others, 2016).

Description of the Study Area

The drainage area of the Herring River watershed in Wellfleet, Mass., at the dike on Chequessett Neck Road (U.S. Geological Survey [USGS] station 011058798) on Cape Cod, is not precisely defined because the contributing groundwater drainage area is not coincident with the surface-water drainage area (Masterson, 2004) and this basin is groundwater dominated (LeBlanc and others, 1986). The surface-water drainage area is approximately 28.5 km^2 (fig. 1) based on the USGS StreamStats application (U.S. Geological Survey, 2015) for Massachusetts. The groundwater contributing area for the Herring River has been simulated by use of a three-dimensional numerical model (MODFLOW) to be approximately 19.1 km^2 (Carlson and others, 2017a, b). In the interpretation of this simulation, the kettle ponds in the northwestern part of the surface water drainage area are not included in the groundwater contributing area.

The Herring River watershed contains a 6-km^2 (600-ha) estuarine marsh complex that is the largest diked wetland system on Cape Cod. The watershed was diked off from the ocean in 1909, resulting in greatly restricted tidal flushing (Portnoy and Allen, 2006). There are four tributaries (fig. 1) draining subbasins in the Herring River: Bound Brook, Duck Harbor, Mill Creek, and Pole Dike Creek; the four subbasins are briefly described in National Park Service and others (2016). The dike restricts tidal amplitude from about 2.1 m seaward to 0.5 m landward of the structure (Portnoy and Allen, 2006). The dike was intended to control mosquitoes, create additional developable land, and provide for road construction. After the original dike construction, widespread ditching, straightening, and channelizing of the meandering creeks effectively drained most of the remaining salt marshes (National Park Service and others, 2016). Between 1929 and 1933, a golf course was constructed, partly on what had previously been part of the Mill Creek (tributary to the Herring River) flood plain. Additionally, several houses have been constructed in the former flood plain.

The dike structure is an earthen dam about 0.15 kilometer (km) in length that contains a culvert with three approximately 4-square-meter rectangular sluiceways in the center of the dike. Within two of the three sluiceways (center and northwestern sluiceways), hydraulic pressure-controlled flapper gates permit ebb discharge and close following an ebb tide, thereby restricting seawater flow upstream during flood tides (Portnoy and Allen, 2006). The third sluiceway (southeastern sluiceway) is a fixed gate that is partially open. This sluiceway allows ebb discharge and is the only sluiceway that allows seawater to flow upstream during flood tides. With the current [2023] dike configuration, seawater travels upstream about 1,000 m into the estuary and marsh complex (Portnoy and Allen, 2006). The dike structure results in tidal asymmetry such that flood tides average 7.2 hours and ebb tides average 5.2 hours during each complete cycle. The tidal cycle in the ocean is consistent with semidiurnal tides (average periodicity of 12.4 hours) for the Gulf of Maine (Garrett, 1972).

Before diking, the tidal flats and low marsh areas were dominated by *Spartina alterniflora* (saltmarsh cordgrass), and the high marsh area was dominated by *Spartina patens* (salt meadow cordgrass). After diking, that vegetation was replaced by brackish and freshwater species, such as *Scirpus* spp. (sedges), *Typha* spp., forbs, shrubs, and grasses (Roman, 1987). Diking also resulted in the establishment of invasive plant species in the Herring River watershed (Smith, 2007; National Park Service and others, 2016) and negatively affected the populations of many fish, shellfish, and other invertebrates, birds, mammals, reptiles, and amphibians (National Park Service and others, 2016).

The mean annual temperature observed at the meteorological station in Truro, which is 5.85 km northeast from the Herring River monitoring station, was 12.3 degrees Celsius (°C) from October 2004 through September 2017 (Western Regional Climate Center, 2018). Mean monthly air temperature is usually between 1 and 4 °C from December through February and between 21 and 24 °C from June through August. The mean annual precipitation near Truro was 121 centimeters (cm) for the period January 1983 to December 2017 (National Atmospheric Deposition Program, 2018). Precipitation is fairly evenly distributed among months and generally averages between 80 and 120 millimeters (mm) each month but can be highly variable in any given month (from less than [<] 10 to more than [>] 130 mm). Groundwater recharge on Cape Cod is about 45 percent of total annual precipitation (LeBlanc and others, 1986).

Various characteristics of the basin, as defined by the surface-water drainage area, are described in the USGS StreamStats application (U.S. Geological Survey, 2015). The watershed is entirely underlain by glacially derived

coarse-grained stratified drift. Forests cover 71 percent of the watershed surface area, wetlands cover 15 percent, ponds cover 4.6 percent, and developed land (largely the suburban town of Wellfleet) occupies about 13.2 percent. percentages add up to >100 percent because some of the forested land is also classified as wetlands. About 3 percent of the developed land is classified as impervious surface. The mean watershed elevation is 14.4 m, and the total length of all mapped streams (1:24,000-scale) in the watershed is 31.2 km.

In 2021 and 2022, sea water breached the beach and dune system that had kept sea water out of Duck Harbor throughout this and previous study periods, and water quality measurements recorded approximately 1.6 km upstream from the beach detected the presence of this sea water in the Herring River (Tim Smith, NPS, written commun., January 24, 2023). This breaching is associated with rising sea level and is expected to occur more frequently with future increases in sea level during most high monthly spring tides.

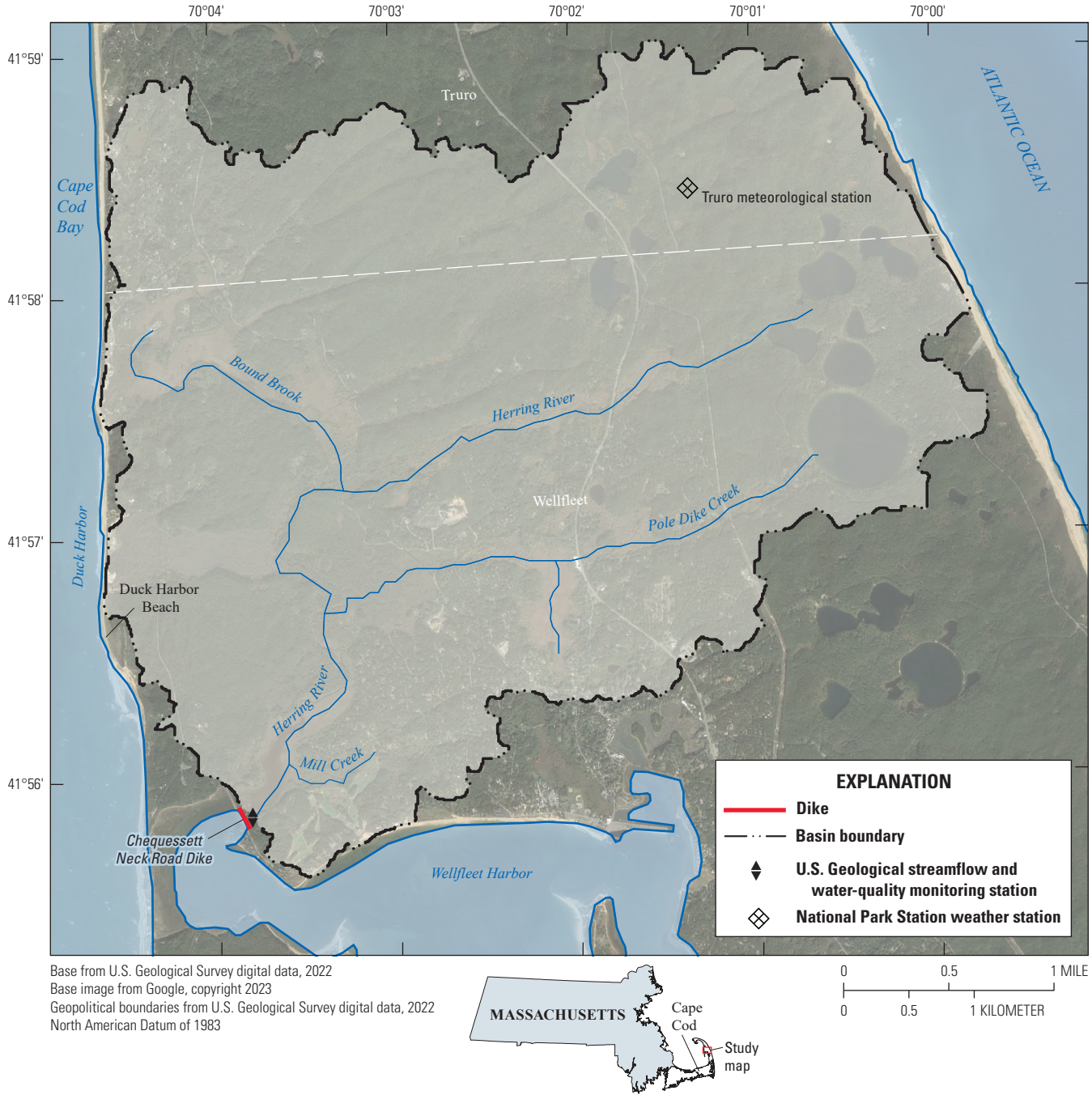

Figure 1. Map showing the Herring River in Wellfleet, Massachusetts, on Cape Cod, showing the watershed basin boundary, monitoring stations, and tributaries.

Purpose

The purpose of this study was to characterize the natural variability in nutrient and suspended sediment concentrations in flood tide and ebb tide waters at the dike currently [2023] installed on the Herring River at Chequessett Neck Road in Wellfleet in relation to environmental variables before the removal of the dike so that this baseline could be used to assess whether removal results in significant changes. This report includes time series of nutrient concentration data from approximately twice monthly sampling of flood and following ebb tides from June 2020 to December 2021 and nutrient data collected during previous USGS studies. These data are discussed in terms of seasonal variations, differences between flood and ebb tide concentrations, and differences between spring, neap, and midamplitude tides. Ancillary time series for air temperature, precipitation, calculated runoff, solar radiation, sea level, nutrient concentrations in Wellfleet Harbor, and atmospheric deposition of nitrogen are also included. Finally, the results of correlation analyses between nutrient concentrations and the ancillary variables are discussed.

This information is intended for use by resource managers at the Cape Cod National Seashore to facilitate planned adaptive management during phased dam removal and reconstruction. Specifically, the time series data provide a range of observed nutrient, dissolved organic carbon, and suspended sediment concentrations over time and a basis for discussion of variation in constituent concentrations in relation to season and environmental characteristics.

Methods

Collection and Processing of Discrete Water Quality Samples

Collection and processing of discrete water quality samples in the current [2023] study followed USGS protocols (U.S. Geological Survey, variously dated). In a previous study, flow-weighted composite samples were collected to obtain samples with nutrient concentrations that were representative of two successive flood or ebb tides (Huntington and others, 2021). Estimation of discharge was not possible in the current [2023] study owing to limitations in project resources; therefore, discrete samples were collected at predetermined times following the beginning of flood and ebb tides. Samples collected at these times were considered to be the most representative of flow-weighted composite concentrations based on analyses comparing discrete samples collected periodically over complete tidal cycles compared with flow-weighted samples where subsamples were collected into a single container over a tidal cycle as described in Huntington and others (2021).

Constituent concentrations varied substantially during tidal cycles and generally followed systematic patterns. Concentrations usually reached a maximum at the end of the ebb tide and the beginning of the flood tide, then declined rapidly to a minimum at the middle of the flood tide, remained near this minimum until early to mid-ebb tide, after which they increased rapidly. Because of this variation in concentration over tidal cycles, discrete grab samples would be representative of the tidal average concentrations if they were collected at times where concentrations were usually similar to the flow-weighted composite samples. Huntington and others (2021, fig. 3) illustrates how nutrient (NH_4, total phosphorus [TP], orthophosphate, and total nitrogen [TN]) concentrations calculated from flow-weighted composite sampling differ from measured individual discrete samples over one sequence of flood followed by ebb tide. The concentrations of orthophosphate on the flood tide were exceptions to this general pattern during the February and May samplings, over which concentrations varied more than during other sequences.

Beginning on February 2, March 22, May 12, and November 4, 2016, samples were collected every 30 minutes for a flood and following ebb tide, and each sample was analyzed for nutrient concentrations. The flow-weighted mean concentrations were calculated from the paired discharge and concentration data. To determine a time following the beginning of the flood or ebb tide to collect a single grab sample that would be most representative of the flow-weighted mean concentration a two-step procedure was used.

In the first step, second order polynomial equations were fit for concentration (x axis) versus time (y axis) for each nutrient for flood and ebb periods. These equations were then solved for the times associated with the calculated flow-weighted mean concentrations. The average times in hours and minutes from the start of each tide from the four dates were calculated for each nutrient. The coefficients of variation for the times associated with the calculated flow-weighted mean concentrations were 12 percent on the flood tide and 16 percent on the ebb tide. The times chosen for sample collection were based on the average times determined for TN and TP. The times based on the polynomial solutions were incremented by 3 minutes for the flood and 6 minutes for the ebb to account for the fact that the first samples were collected after a fixed volume had flowed past the gage (Huntington and others, 2021). The sampling times were determined to be 3 hours and 14 minutes after the start of the flood and 2 hours and 37 minutes after the start of the ebb tide. The beginning of each tide was determined from the time when the surface velocity changed from positive to negative (start of the flood) and negative to positive (start of the ebb). Surface-water velocity was measured by using a contact-free Sommer Messtechnik GmbH RG–30 radar sensor (Sommer Mess Systemtechnik, 2014) on the upstream side (marsh side) of the dike as described in Huntington and others (2021).

In the second step, second order polynomial equations were then fit for time (x axis) versus concentration (y axis) for each nutrient for flood and ebb periods and solved for the concentration associated with the average times calculated above. These concentrations were compared with the calculated flow-weighted mean concentrations to compute the percent error in each case. The errors between the concentrations derived

from the polynomials and those derived from the calculated flow-weighted average concentrations generally were between 2 and 10 percent on the ebb tide. The errors were substantially larger on the flood tide ranging from less than or equal to (≤) 20 percent for TN, TP, total dissolved phosphorus (TDP), and orthophosphate to between 50 and 136 percent for NH_4, nitrate (NO_3) plus nitrite (NO_2), and silica (SiO_2). For the ebb tide, the differences between the calculated flow-weighted mean concentrations and the concentrations determined from sampling at 2 hours and 37 minutes after the start of the tide were 7, 14, 5, 1, 4, 34, and 6 percent for TN, TP, TDP, orthophosphate, NH_4, NO_3, and SiO_2, respectively. For the flood tide these differences from sampling at 3 hours and 14 minutes after the start of the tide were 12, 25, 4, 2, 28, 85 and 122 percent for TN, TP, TDP, orthophosphate, NH_4, NO_3, and silicon, respectively.

To quantify differences in concentrations between sampling at fixed times following the beginning of the flood and ebb tides compared with the method of flow-weighted composite sampling in the previous study the data were compared for the same seasonal periods. All constituents sampled between mid-June 2020 to mid-December 2021 were compared with previous data from mid-June 2016 to mid-December 2017 except dissolved organic carbon (DOC) and total dissolved nitrogen (TDN) data from the current [2023] study. Shorter sampling periods were used for the comparison of DOC and TDN because available data records had shorter periods of record.

At the Chequessett Neck Road monitoring station (USGS station 011058798) samples were collected approximately every 2 weeks on flood tides and the subsequent ebb tides from June 2020 through December 2021. Samples were usually collected from spring tides and from neap tides each month. Tides were judged to be spring tides if they were among the five highest amplitude tides and neap tides if they were judged to be among the four lowest amplitude in a given month. In some months, it was not possible to collect samples during spring or neap tides or there were no obvious spring or neap tides, so samples were collected from midamplitude tides.

Sample collections were made using a peristaltic pump through tubing to an orifice located approximately 10 cm above the base of the concrete sluiceway and in the same location as samples were collected as described in Huntington and others (2021). The ISCO pump used in the current [2023] study (Teledyne ISCO, 2015) has been shown to sample sediment concentrations isokinetically (Bogen, 2004). The pump was actuated manually, following U.S. Geological Survey protocol (app. 2; Francesca Wilde, USGS, written commun., 2009), a minimum of 1 liter (L) of water was pumped through the capsule filter to rinse it prior to collection of any samples. After rinsing the raw water exiting the pump was first filtered using 0.45-micrometer (µm) capsule filters for dissolved constituents (NH_4, NO_3 plus NO_2, orthophosphate, TDP, and SiO_2). The filtrate for these constituents were collected in amber opaque 125-milliliter (mL) polyethylene bottles. The raw water exiting the pump was then used to fill amber opaque 125-mL polyethylene bottles for total nitrogen (TN) and total phosphorus (TP) and a sample for filtration using a syringe filter. TDN includes NH_4, NO_3 plus NO_2, and dissolved organic nitrogen. Particulate organic nitrogen (PON) was calculated as TN minus TDN.

A 0.45-µm Supor membrane syringe filter was used to filter samples for DOC and TDN. The syringe filter was used for TDN and DOC because the cartridge filters have been shown to leach organic nitrogen (app. 3; Sorenson and others, 2018; Francesca Wilde, USGS, written commun., 2017). Samples for DOC were collected and stored in 125-mL amber glass bottles. Samples for TDN were collected in amber opaque 125-mL polyethylene bottles. Finally, raw water exiting the pump was then used to fill 3–L bottles for measurement of suspended sediment concentration. All nitrogen, phosphorus, and SiO_2 samples were pumped into amber opaque 125-ml polyethylene bottles and were chilled until analyzed. DOC samples were pumped into 125-mL amber glass bottles. All samples with the exception of the 3–L samples were chilled until analyzed.

Analytical Methods and Quality Assurance

Concentrations of NO_3 plus NO_2, NH_4, TDN, TDP, SiO_2, orthophosphate, TN, and TP were analyzed at the Center for Coastal Studies Laboratory in Provincetown, Mass. DOC was analyzed at the U.S. Forest Service Northern Research Station in Parsons, W.Va. The 3–L samples for suspended sediment concentration were shipped to the USGS Kentucky Sediment Laboratory in Louisville, Ky., for analysis. The analytical methods used for water quality analysis, USGS parameter codes, method references, and minimum detection limits for samples collected at water quality-monitoring stations on the Herring River are summarized in table 1.

Laboratory quality assurance protocols included the analysis of standard reference materials, field replicates, field blanks, and laboratory blanks and reasonable range checks. All water quality and quality assurance data for the current [2023] study are published in the U.S. Geological Survey National Water Information System (NWIS) database (U.S. Geological Survey, 2022). Laboratory analyses of standard reference materials for nutrients and DOC consistently met the data quality objectives established for the current [2023] study. The data quality objectives were relative percent differences (RPDs) of <20 percent. Analysis of field sequential replicate samples shows that median RPD values between the replicates and the corresponding environmental samples for all constituents were usually substantially less than the data quality objectives of ±20 percent.

Field blank results indicated that, in most cases, blank analyte concentrations were below minimum reporting levels or substantially lower than the lowest environmental sample for nutrients, except for concentrations of NH_4. The median value for the concentration of NH_4 field blanks was 0.0033 milligrams per liter (mg/L) as nitrogen, which was

Table 1. Constituents analyzed for water quality from samples collected at water quality monitoring stations on the Herring River, Wellfleet, Massachusetts.

[U.S. Geological Survey (USGS) parameter codes are from the National Water Information System (NWIS) at U.S. Geological Survey (2022). mg/L, milligram per liter; N, nitrogen; SiO_2, silica; P, phosphorus; C, carbon; °C, degree Celsius]

Constituent and unit	Analytical method	USGS parameter code	Method reference	Minimum detection limit
Ammonia, filtered, in mg/L as N	Automated phenate colorimetry	00608	U.S. Environmental Protection Agency (1993)	0.0014
Nitrate plus nitrite, filtered, in mg/L as N	Automated cadmium reduction and colorimetry	00631	Zhang and others (1997)	0.0007
Silica, filtered, in mg/L as SiO_2	Automated segmented flow, molybdate blue formation and colorimetry	00955	Zhang and Berberian (1997)	0.006
Orthophosphate, in mg/L as P	Ascorbic acid method, molybdenum blue colorimetry	00671	Zimmerman and Keefe (1997)	0.0006
Total dissolved phosphorus, filtered, in mg/L as P	Alkaline-persulfate digestion, continuous flow colorimetry	00666	Patton and Kryskalla (2003)	0.003
Total nitrogen, unfiltered, in mg/L as N	Alkaline-persulfate digestion, continuous flow colorimetry	62855	Patton and Kryskalla (2003)	0.007
Total dissolved nitrogen, filtered, in mg/L as N	Alkaline-persulfate digestion, continuous flow colorimetry	62854	Patton and Kryskalla (2003)	0.007
Total phosphorus, unfiltered, in mg/L as P	Alkaline-persulfate digestion, continuous flow colorimetry	00665	Patton and Kryskalla (2003)	0.003
Dissolved organic carbon, in mg/L as C	High-temperature catalytic oxidation, nondispersive infrared detection	00681	Sugimura and Suzuki (1988)	0.24
Suspended sediment concentration, in mg/L	Sediment concentration by filtration	80154	Guy (1969); ASTM International (1999)	1

above the detection limit but substantially lower than all but two environmental samples that were also below detection limits. Analyses of laboratory-prepared deionized water blanks showed that there was no detectable contamination of samples within the laboratory for any constituent.

Data Collected at the Chequessett Neck Road Monitoring Station in Previous Projects

For analyses in the current [2023] study, nutrient concentration data were aggregated with data from two previous studies. The first study included data collected from November 2015 to September 2017 that was described in Huntington and Spaetzel (2020) and Huntington and others (2021) and are published in NWIS (U.S. Geological Survey, 2022). The second study included data from October 2017 to September 2018. The data from the second study are published in NWIS (U.S. Geological Survey, 2022). Data collection during these previous projects used flow-weighted composite sampling. The data from these previous studies were included in this analysis to increase the period of record to maximize the characterization of the baseline before the removal of the dike.

Measurements to determine if sampling from a single point in one sluiceway was representative of the total volume of water flowing during ebb tides were discussed in Huntington and others (2021). The results of that comparison indicated that, for certain constituents, the automated point-sampling is not fully representative of the water in the cross section and introduces some error. The data from these analyses comparing point sampling to equal-width interval sampling generally met a data quality objective of <20 percent RPD for most analytes (TN, TP, orthophosphate, NO_3 plus NO_2, and SiO_2), but the RPD was >20 percent for other analytes (NH_4 and TDP; Huntington and others, 2021).

Ancillary Environmental Data

Ancillary environmental data were compiled to investigate whether they could explain observed variations in nutrient concentrations. Monthly average surface maximum and minimum air temperature, precipitation, and downwelling surface shortwave radiation were obtained from the gridMET dataset (Abatzoglou, 2013), a dataset of daily high-spatial resolution (about 4-km, 1/24th degree [°]) surface meteorological data covering the contiguous United States. Data from the spatial domain defined by the coordinates that encompassed

the Herring River watershed area were retrieved using the area of interest and getGridMet functions in R (Climatology Lab, 2017). The spatial coordinates were $x_{min} = -70.0844$, $x_{max} = -69.97111$, $y_{max} = 41.97389$, $y_{min} = 41.92333$, where x refers to longitude and y refers to latitude. Mean temperature was calculated as the simple average of minimum and maximum temperatures. Daily meteorological data were aggregated to monthly data.

Runoff from the Herring River watershed was calculated using the Thornthwaite water balance model that partitions precipitation inputs to evapotranspiration, runoff, or storage by using a monthly accounting procedure described in McCabe and Markstrom (2007). Inputs to the model are the mean monthly surface air temperature (in degrees Celsius), monthly total precipitation (in millimeters), and latitude (in decimal degrees) of the location of interest. The temperature and precipitation inputs were derived from gridMET as described above. The latitude was input as 42°. The model uses other input parameters defined as follows: runoff factor, 50 percent; direct runoff factor, 5 percent; soil moisture storage capacity, 150 mm; rain temperature threshold, 3.3 °C; snow temperature threshold, −10 °C; maximum melt rate, 50 percent. The monthly environmental variables and runoff data are published in Huntington (2023).

Monthly mean sea level data for Woods Hole, Mass. (National Oceanic and Atmospheric Administration [NOAA] station 8447930) were obtained from NOAA (2022a). Mean monthly surface ocean water temperature was obtained from NOAA station 44090 (41.840 N −70.329 W; NOAA, 2022c) supplemented with data from NOAA station 44013 (42.346 N −70.651 W; NOAA, 2022b). Monthly sea level and ocean water temperature data are published in Huntington (2023).

Nutrient concentration data from Wellfleet Harbor station 43 were obtained from the Center for Coastal Studies (2022), which collects samples under the Cape Cod Bay Monitoring Program from the ocean surface once in May and October and twice per month from June through September. Nutrient concentration data obtained from the Center for Coastal Studies are published in Huntington (2023).

Data for atmospheric deposition of nitrogen were obtained from the National Atmospheric Deposition Program station in Barnstable, Mass. (site MA01; National Atmospheric Deposition Program, 2018). This site is 32 km and 218° southwest of the Herring River gage. There are missing data for many months, and the monthly data were only available through December 2020. The NADP uses the following completeness criteria for data acceptance:

- Criterion 1, there must be valid samples for at least 75 percent of the summary period.
- Criterion 2, for at least 90 percent of the summary period there must be precipitation amounts (including zero amounts) either from the rain gage or from the sample volume.
- Criterion 3, there must be valid samples for at least 75 percent of the total precipitation amount reported for the summary period.

Twenty-seven out of 61 months in the record from November 2015 to December 2020 had completeness criteria that were acceptable and were well distributed over the record. Data for atmospheric deposition of nitrogen are published in Huntington (2023).

Correlation Analyses

Kendall's rank correlation tests were run between nutrient concentrations on the ebb tide and environmental variables including precipitation, surface air temperature, runoff, downwelling shortwave radiation, ocean water temperature, mean sea level, and atmospheric deposition of NO_3 plus NO_2 and NH_4 (Huntington, 2023). Correlation tests were run in Tibco Spotfire software, and the results were summarized based on significance probability levels of <0.01, <0.05 and <0.1; p-values greater than 0.1 were not significant.

Results

Differences in Concentration Based on Sampling Methodologies

The method of sample collection in the current [2023] study involved sampling at a fixed time following the beginning of a single flood or ebb tide and not the flow-weighted composite sampling following two successive flood or ebb tides of the previous studies (Huntington and others, 2021). The analysis showed that it is likely that there would be small differences between methods in measured concentrations on the ebb tides and somewhat larger differences on the flood tides. The larger RPDs are generally associated with low concentrations on the flood tides.

Differences in constituent concentrations between the previous studies and this study could be related to differences in environmental conditions between these periods or differences in sampling methodologies. The following paragraph describes the relationships between selected nutrient concentrations and environmental variables that could explain part of the differences in concentrations between periods. The description of differences in the next paragraph assumes that the differences are explained solely by the different methods.

Average constituent concentrations were higher in the previous study that used flow-weighted composite sampling (Huntington and others, 2021; U.S. Geological Survey, 2022) compared with the current [2023] study that used fixed time sampling for NH_4, TP, silicon, and DOC on the flood and NH_4, TP, TDP, silicon, and DOC on the ebb tides (table 2). Constituent concentrations generally were higher in the current [2023] study using the fixed time sampling method

Table 2. Comparison of constituent concentrations collected at the Herring River at Chequessett Neck Road monitoring station in Wellfleet, Massachusetts.

[The data were collected over the same seasonal periods for both previous studies using flow-weighted composite sampling (Huntington and others, 2021; U.S. Geological Survey, 2022) and the current [2023] study using sampling at fixed times (this report) following the beginning of the flood or ebb tide]

Analyte	Flood		Ebb	
	Previous	Current	Previous	Current
Nitrite plus nitrate				
Number of samples	63	36	59	38
Mean, in milligrams per liter	0.0071	0.007	0.0152	0.0235
Standard error of the mean, in milligrams per liter	0.0006	0.00095	0.00135	0.00401
Relative percent difference between the mean values, in percent		1.42	43	
Ammonium				
Number of samples	63	36	59	38
Mean, in milligrams per liter	0.043	0.007	0.064	0.024
Standard error of the mean, in milligrams per liter	0.0076	0.0009	0.0086	0.004
Relative percent difference between the mean values, in percent		144		91
Total dissolved nitrogen				
Number of samples	29	28	28	29
Mean, in milligrams per liter	0.28	0.26	0.36	0.34
Standard error of the mean, in milligrams per liter	0.012	0.018	0.015	0.037
Relative percent difference between the mean values, in percent		7.4		5.7
Total nitrogen				
Number of samples	63	37	61	37
Mean, in milligrams per liter	0.42	0.35	0.5	0.43
Standard error of the mean, in milligrams per liter	0.016	0.02	0.029	0.033
Relative percent difference between the mean values, in percent		18		15
Orthophosphate				
Number of samples	63	28	59	25
Mean, in milligrams per liter	0.035	0.055	0.036	0.034
Standard error of the mean, in milligrams per liter	0.0037	0.0114	0.0034	0.0066
Relative percent difference between the mean values, in percent		44		5.7
Total dissolved phosphorus				
Number of samples	63	37	59	38
Mean, in milligrams per liter	0.024	0.028	0.024	0.019
Standard error of the mean, in milligrams per liter	0.002	0.004	0.0018	0.0028
Relative percent difference between the mean values, in percent		15		23
Total phosphorus				
Number of samples	63	37	61	37
Mean, in milligrams per liter	0.053	0.047	0.062	0.038
Standard error of the mean, in milligrams per liter	0.0028	0.0052	0.0036	0.004
Relative percent difference between the mean values, in percent		12		48
Silica				
Number of samples	63	37	59	38
Mean, in milligrams per liter	1.15	0.58	2.37	2.07
Standard error of the mean, in milligrams per liter	0.07	0.068	0.119	0.187
Relative percent difference between the mean values, in percent		65		14

Table 2. Comparison of constituent concentrations collected at the Herring River at Chequessett Neck Road monitoring station in Wellfleet, Massachusetts.—Continued

[The data were collected over the same seasonal periods for both previous studies using flow-weighted composite sampling (Huntington and others, 2021; U.S. Geological Survey, 2022) and the current [2023] study using sampling at fixed times (this report) following the beginning of the flood or ebb tide]

Analyte	Flood		Ebb	
	Previous	Current	Previous	Current
Dissolved organic carbon				
Number of samples	41	29	38	21
Mean, in milligrams per liter	2.98	2.37	4.36	3.79
Standard error of the mean, in milligrams per liter	0.2	0.13	0.37	0.45
Relative percent difference between the mean values, in percent		23		14

compared with the previous studies using flow-weighted composite sampling for orthophosphate and TDP on the flood tide and NO_3 plus NO_2 on the ebb tide (table 2). For TDN, TN, TDP, and DOC, the RPDs in concentrations were <25 percent between methods on the flood and ebb tides (table 2). For NO_3 plus NO_2 and TP on the flood and for orthophosphate and SiO_2 on the ebb, the RPDs in concentrations were <25 percent between methods. For NO_3 plus NO_2 and TP on the ebb and for orthophosphate and silicon on the flood, the RPDs in concentrations were between 43 and 55 percent between methods. For NH_4, the RPDs in concentrations were 144 percent on the flood and 91 percent on the ebb between methods.

The NO_3 plus NO_2 ebb tide concentrations between the two sampling periods were similar except in September through November (app. 1, fig. 1.1). In September 2021, ebb tide NO_3 plus NO_2 concentrations were more than three times greater compared with the early period (2016–17). Runoff in September 2021 was more than four times greater and precipitation was more than two times greater compared with the 2016–17 period (app. 1, figs. 1.2 and 1.3). The October 2020 and 2021 periods also had higher NO_3 plus NO_2 concentrations and higher runoff. These differences in NO_3 plus NO_2 concentrations from the early to the recent periods could be partially explained by increases in precipitation and runoff. The differences in TN and SiO_2 concentrations between periods (app. 1, figs. 1.4 and 1.5) were also associated with greater precipitation and runoff; however, in these cases, the differences generally were between December 2020 through August 2021 (app. 1, fig. 1.3). The possibility that increases in precipitation and runoff may explain part of the differences in these nutrients between the early and recent periods is consistent with the correlations between these nutrients and precipitation and runoff for the complete dataset (discussed in the "Correlations Between Monthly Average Nutrient Concentrations on the Ebb Tide and Corresponding Monthly Average Environmental Variables" section of this report). Differences between other constituents between periods on the ebb tide do not show consistent relations with the environmental variables studied. There were only very small differences in monthly average air temperature (app. 1, fig. 1.6) and monthly average solar radiation (app. 1, fig. 1.7) between the early and recent periods, so it is unlikely that differences in these variables could explain differences in nutrient concentrations.

Variation in Nutrient and Suspended Sediment Concentrations in the Herring River by Season and Tide Direction

Nutrient and suspended sediment concentration varied by season and tide direction in the Herring River during the period of record. Concentrations of NO_3 plus NO_2, NH_4, TDN, TN, SiO_2, and DOC generally were higher on the ebb tide than on the flood tide. By contrast, concentrations of orthophosphate, TDP, and TP were generally similar between flood and ebb tides.

The concentrations of NO_3 plus NO_2 generally varied between 0.003 and 0.01 mg/L on flood tides and between 0.003 and 0.03 mg/L on ebb tides (fig. 2*A*). NO_3 plus NO_2 concentrations were similar between flood and following ebb tides in late summer and early fall, but ebb tide concentrations generally increased from late fall, peaking in winter, and decreasing until summer, whereas flood tide concentrations remained low (fig. 2*A* and *B*). These patterns resulted in distinct seasonal variation in the difference between flood and ebb tide concentration, although this pattern was less pronounced in the current [2023] study than in the previous studies (Huntington and others, 2021; U.S. Geological Survey, 2022). Variation in NO_3 plus NO_2 concentrations between flood and ebb tides during each season shows that ebb tide concentrations were higher than flood tide concentration in all seasons, but the differences were greatest in spring and winter and least in summer (fig. 3). Variation within a season was greatest in summer and winter for the flood tide and in summer for the ebb tide.

The concentrations of NH_4 generally varied between 0.008 and 0.09 mg/L on flood tides and between 0.02 and 1.0 mg/L on ebb tides (fig. 4*A*). Seasonal variation in NH_4 concentrations was substantially more variable than for NO_3 plus NO_2 concentrations. In general, NH_4 concentrations were higher on the ebb tide than on the flood tide, but the seasonal

pattern of these differences was less consistent than for NO_3 plus NO_2 (fig. 4*B*). The differences between flood and ebb tides were small but more consistent in the current [2023] study than in the previously published data (Huntington and others, 2021; U.S. Geological Survey, 2022). In contrast to the patterns observed for NO_3 plus NO_2, NH_4 concentrations on the flood tide tended to be higher in summer and fall and lower in spring and winter (fig. 5).

The period of record for TDN was shorter than for TN, NO_3 plus NO_2, or NH_4 because of potential contamination in the earliest record (November 11, 2015, to July 26, 2017). The concentrations of total TDN generally varied between 0.13 and 0.40 mg/L on flood tides and between 0.20 and 0.5 mg/L on ebb tides (fig. 6*A*). TDN concentrations generally were higher on the ebb tide than the flood tide and higher in late fall and winter than during the spring and summer (fig. 6*B*).

TDN concentrations were higher on the ebb than the flood tide in all seasons but the difference was smallest in summer (fig. 7). Comparing these TDN data with the data for TN indicates that a substantial fraction of TN is particulate organic nitrogen (PON; >0.45 µm) on the flood tide (33 to 57 percent) and ebb tide (25 to 75 percent). The PON fraction was estimated as the difference between TN and TDN. On the flood tide, the PON fraction is higher at higher TDN concentrations, and on the ebb tide, the PON fraction is higher at lower TDN concentrations.

Concentrations of TN generally varied between 0.25 and 0.5 mg/L on flood tides and between 0.25 and 0.7 mg/L on ebb tides (fig. 8*A*). TN concentrations generally were similar between flood and ebb tides in summer and fall but were higher on ebb tides than flood tides in winter and spring (figs. 8*B* and 9). Within-season variation in concentration of TN was greater for ebb tides than flood tides in winter, spring, and fall but smaller in summer. The differences between flood and ebb tides were similar between this and previous studies.

The concentrations of orthophosphate generally varied between 0.007 and 0.09 mg/L on flood and ebb tides (fig. 10*A*). Orthophosphate concentrations generally increased beginning in late spring or early summer, peaked in mid- to late summer, then decreased to minimum concentrations in winter and early spring. These patterns resulted in distinct seasonal variation with a single peak each year. The differences between flood and ebb tide concentrations generally were small, but ebb tide concentrations generally were greater than flood tide concentrations in fall and winter but were similar in spring and summer (figs. 10*B* and 11). In the current [2023] study, there was either little or no difference between ebb and flood, or during high summer concentrations, the flood tide concentrations were usually higher (fig. 10*A* and *B*).

The concentrations of TDP generally varied between 0.006 and 0.05 mg/L on flood and ebb tides (figs. 12*A* and 13). The seasonal variation in TDP generally was quite similar to that observed for orthophosphate for flood and ebb tides (figs. 10*B* and 12*B*). The differences between flood and ebb tide concentrations generally were small, but ebb tide concentrations generally were greater than flood tide concentrations in fall and spring but similar in summer and winter (fig. 13).

The concentrations of TP generally varied between 0.03 and 0.09 mg/L on flood and ebb tides (figs. 14*A* and 15). Flood and ebb tide TP concentrations generally increased beginning in late spring, peaked in late summer, then decreased to minimum concentrations in winter (fig. 14*A*). These patterns resulted in seasonal variation with a single peak each year but with more within-season variability than observed for orthophosphate (fig. 10*B*). Ebb tide concentrations were slightly higher than flood tide concentrations in spring and fall but were very similar summer and winter, albeit with somewhat larger interquartile ranges (fig. 14*B* and 15). In the current [2023] study there were either little or no differences between ebb and flood or, during summer when concentrations were highest, the concentrations on the flood tide were usually higher.

The concentrations of SiO_2 generally varied between 0.5 and 1.5 mg/L on flood tides and between 1.5 and 3.0 mg/L on ebb tides (fig. 16*A*). SiO_2 concentrations were higher on the ebb tide than the flood tide in all seasons by a factor of two or more (figs. 16 and 17). There were no consistent seasonal differences in silica concentrations between flood and ebb tides.

The concentrations of DOC generally varied between 1.8 and 3.5 mg/L on flood tides and between 2.0 and 5.0 mg/L on ebb tides (fig. 18*A*). DOC concentrations generally were higher on the ebb tide than the flood tide in all seasons (figs. 18*B* and 19). The largest difference was in the spring, followed by the summer and winter, and the smallest difference was in the fall (fig. 19). DOC concentrations were highest in spring and summer and lowest in winter for flood and ebb tides (figs. 18*A* and 19), resulting in a seasonal pattern having one peak and one trough each year.

The period of record for suspended sediment concentration was from July 2020 through December 2021 and was insufficient to establish seasonal patterns. Suspended sediment concentrations were low and generally varied between 2 and 9 mg/L during flood and ebb tides (fig. 20*A*). In most cases, the differences between flood and ebb concentrations were <5 mg/L; however, there were six instances in summer and fall 2021 where ebb concentrations were more than 10 mg/L greater than flood concentrations and two instances in spring and summer 2021 where flood concentrations were more than 10 mg/L greater than ebb concentrations (fig. 20*B*). In spring, summer, and fall 2021, there were a total of seven ebb and two flood samples with suspended sediment concentrations in the range of 20 to 40 mg/L (fig. 20*A*). In most of these cases, the ebb samples had substantially higher suspended sediment concentrations than the flood samples (fig. 20*B*).

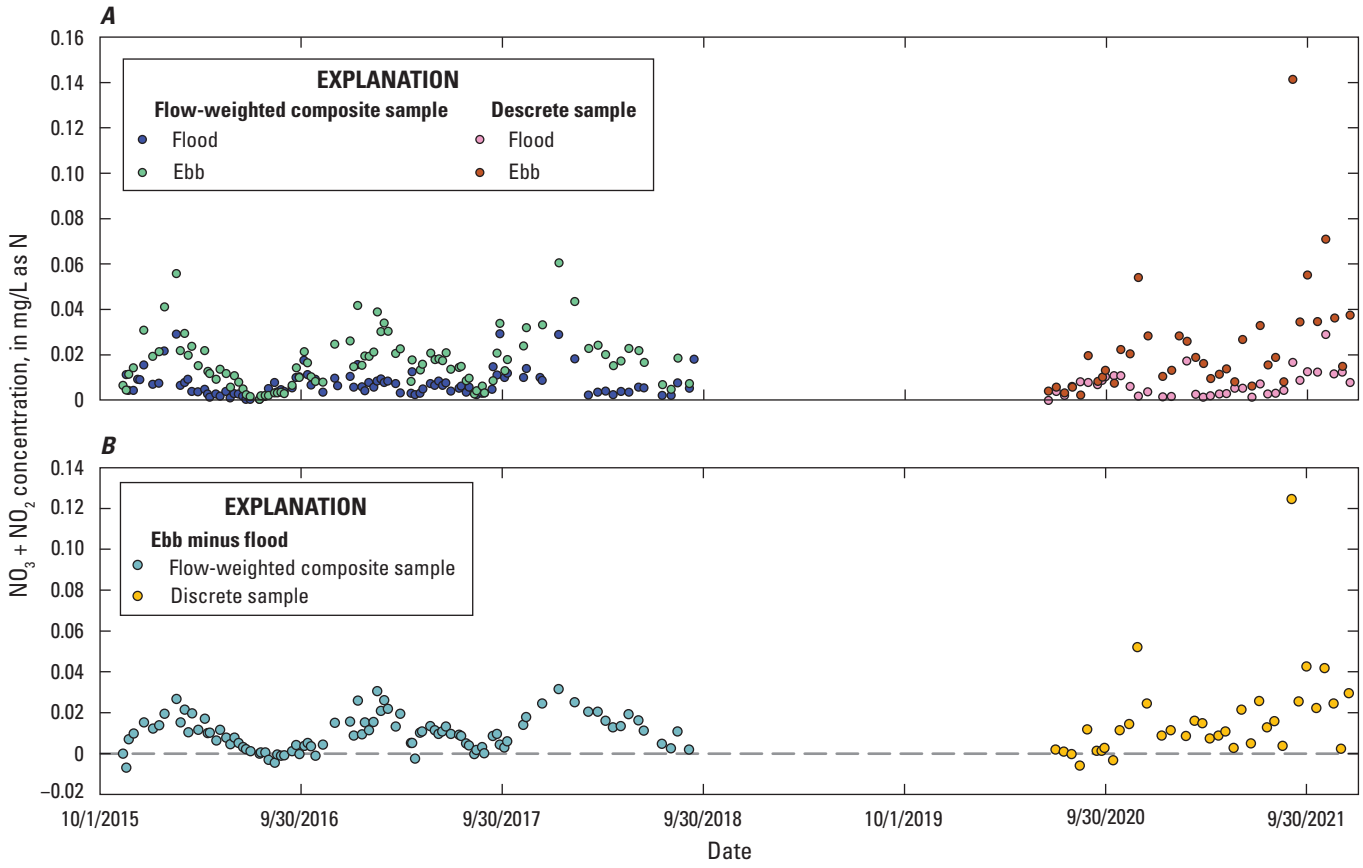

Figure 2. Graphs showing nitrate plus nitrite concentrations in the Herring River at Chequessett Neck Road in Wellfleet, Massachusetts, for flow-weighted composite samples from sequential flood and ebb tides, November 2015 through September 2018 and discrete samples from sequential flood and ebb tides from June 2020 through December 2021. *A*, Concentration measurements and *B*, the difference (ebb minus flood) in concentrations. $NO_3 + NO_2$, nitrate plus nitrite; mg/L as N, milligram per liter as nitrogen.

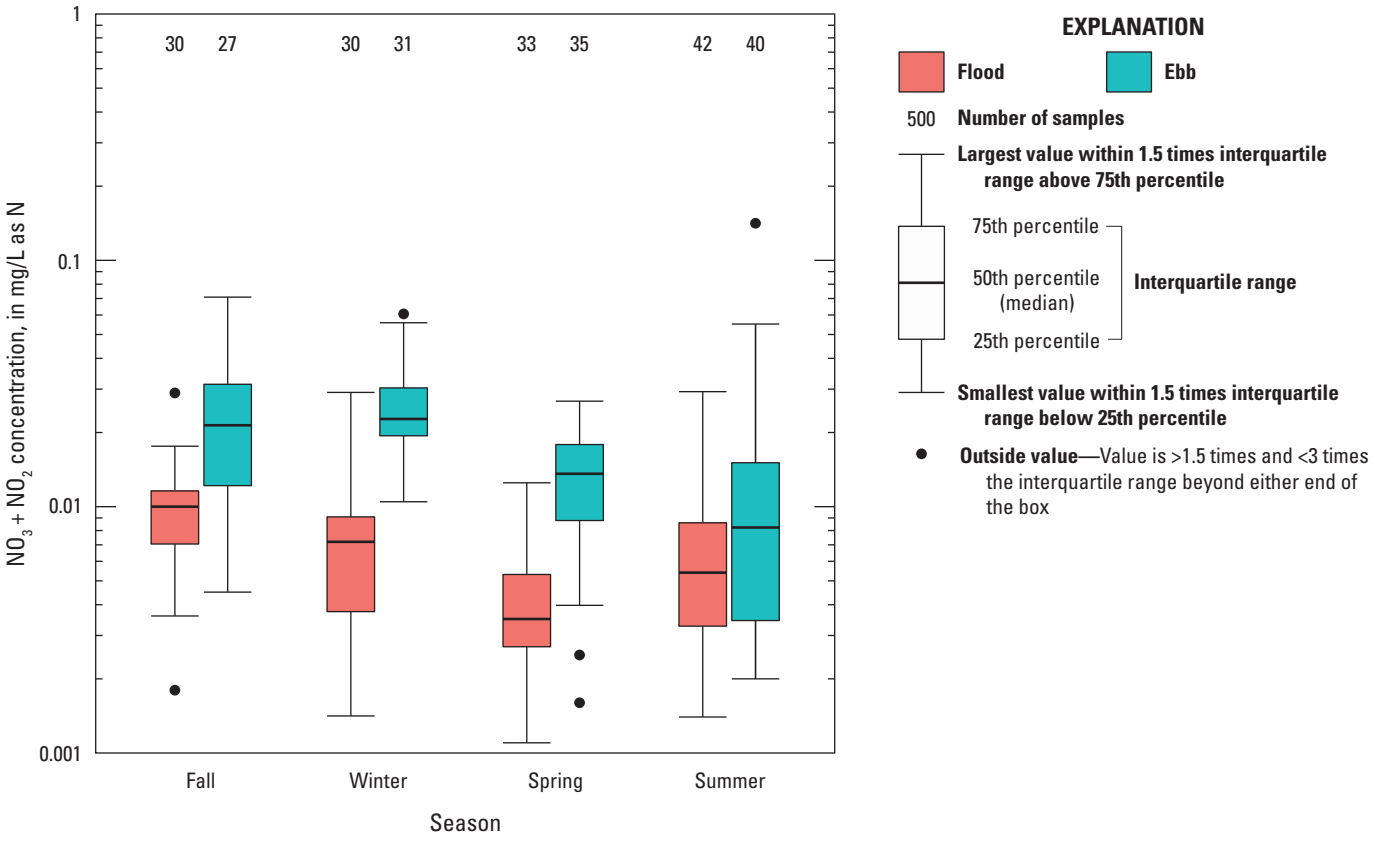

Figure 3. Boxplot showing nitrate plus nitrite concentrations in the Herring River at Chequessett Neck Road in Wellfleet, Massachusetts, for flow-weighted composite samples from sequential flood and ebb tides from November 2015 through September 2018 and discrete samples from sequential flood and ebb tides from June 2020 through December 2021 across seasons and tidal periods. $NO_3 + NO_2$, nitrate plus nitrite; mg/L as N, milligram per liter as nitrogen; >, greater than, <, less than.

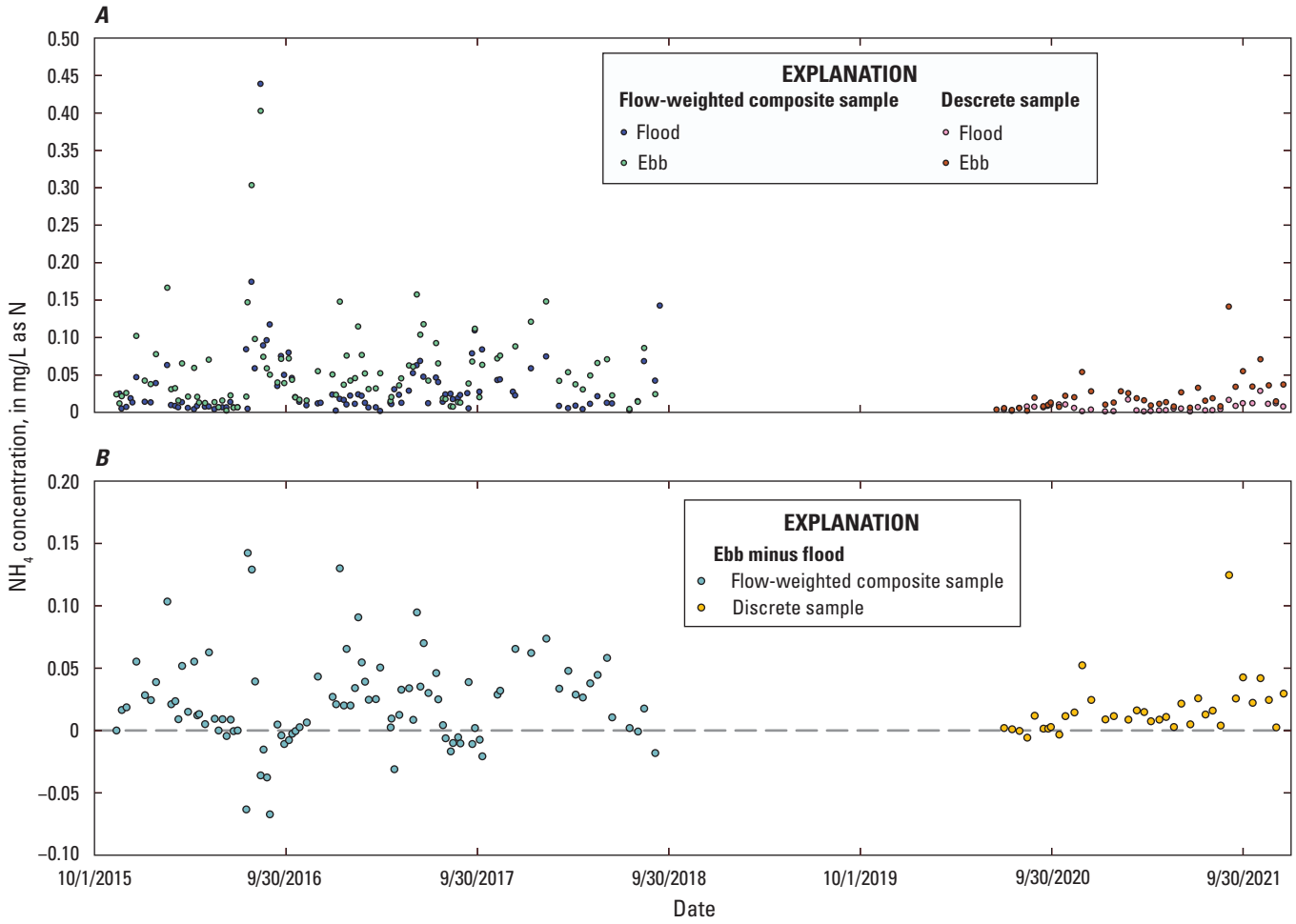

Figure 4. Graphs showing ammonium concentrations in the Herring River at Chequessett Neck Road in Wellfleet, Massachusetts, for flow-weighted composite samples from sequential flood and ebb tides from November 2015 through September 2018 and discrete samples from sequential flood and ebb tides, June 2020 through December 2021. *A*, Concentration measurements and *B*, the difference (ebb minus flood) in concentrations. $NO_3 + NO_2$, nitrate plus nitrite; mg/L as N, milligram per liter as nitrogen.

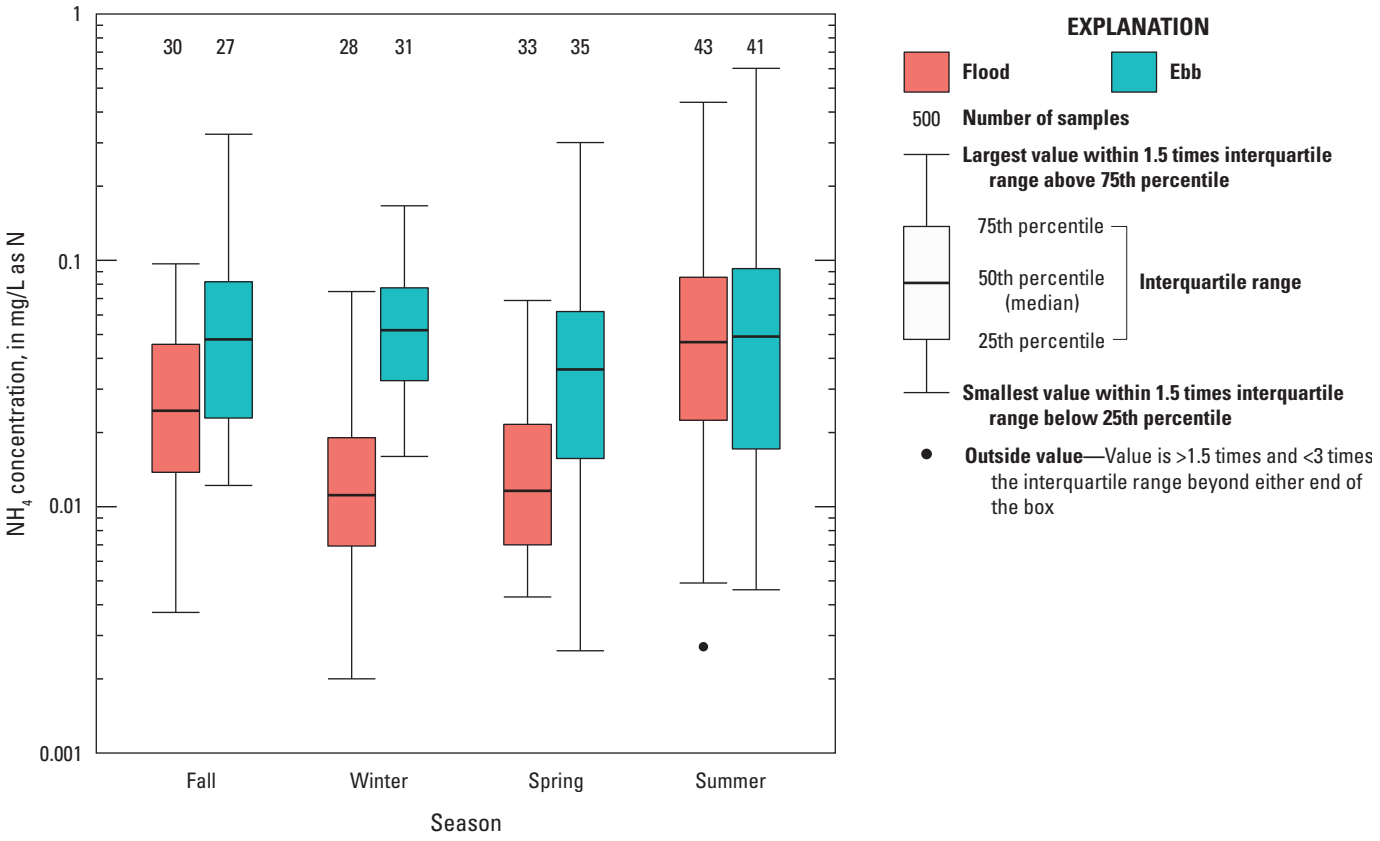

Figure 5. Boxplot showing ammonium concentrations in the Herring River at Chequessett Neck Road in Wellfleet, Massachusetts, for flow-weighted composite samples from sequential flood and ebb tides from November 2015 through September 2018 and discrete samples from sequential flood and ebb tides from June 2020 through December 2021 across seasons and tidal periods. mg/L as N, milligram per liter as nitrogen; >, greater than, <, less than.

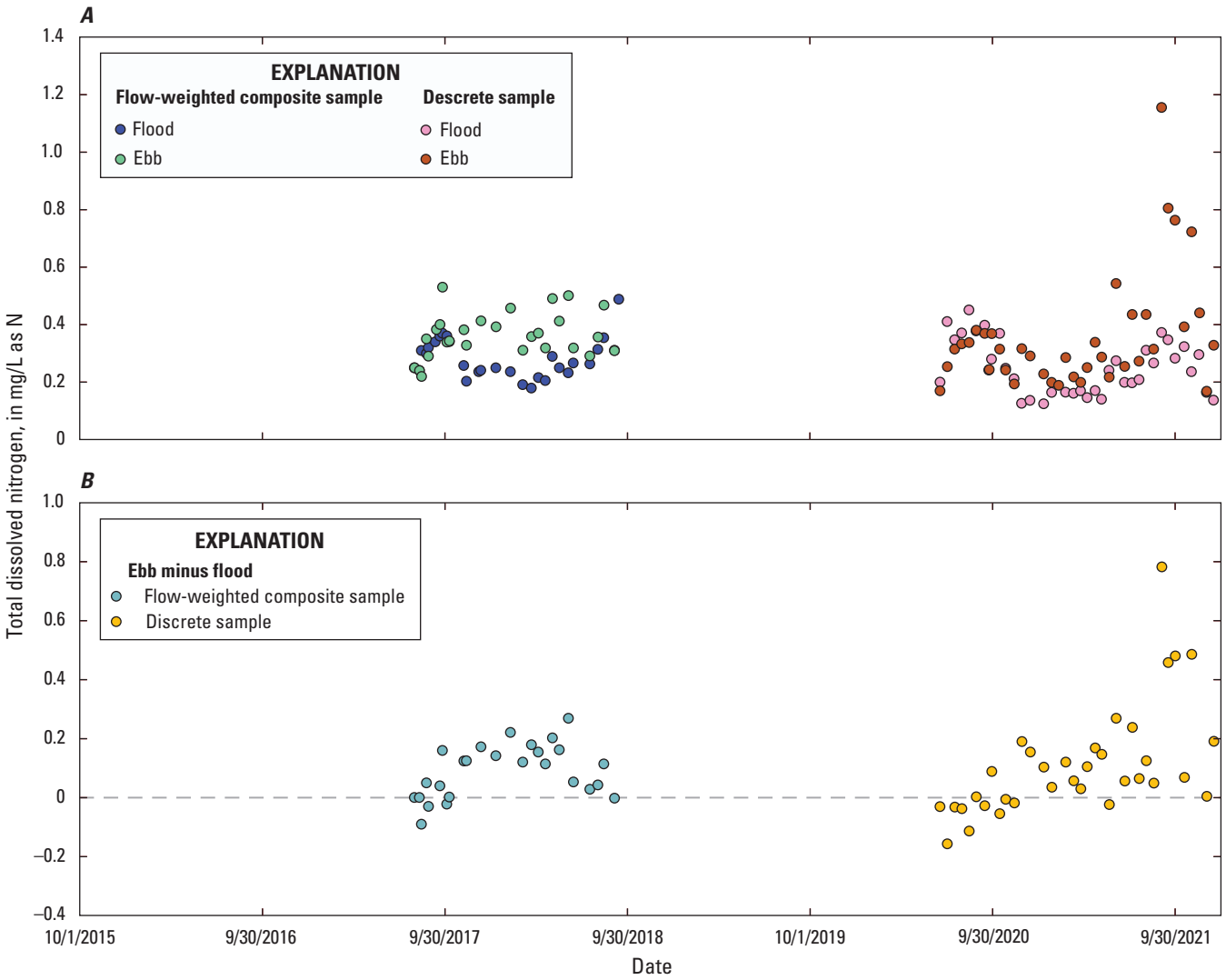

Figure 6. Graphs showing total dissolved nitrogen concentrations in the Herring River at Chequessett Neck Road in Wellfleet, Massachusetts, for flow-weighted composite samples from sequential flood and ebb tides from July 2017 through September 2018 and discrete samples from sequential flood and ebb tides, June 2020 through December 2021. *A*, Concentration measurements and *B*, the difference (ebb minus flood) in concentrations. mg/L as N, milligram per liter as nitrogen.

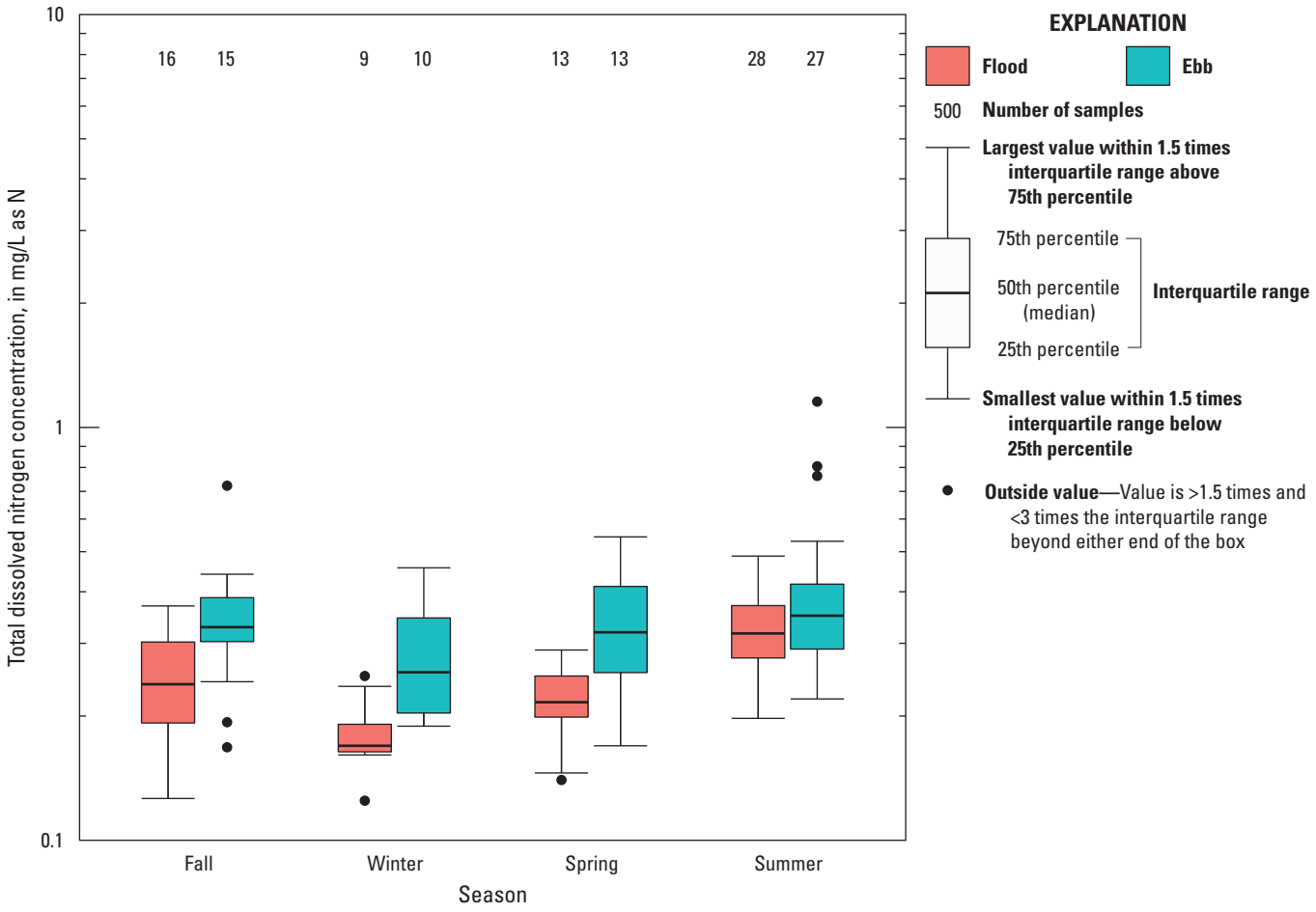

Figure 7. Boxplot showing total dissolved nitrogen concentrations in the Herring River at Chequessett Neck Road in Wellfleet, Massachusetts, for flow-weighted composite samples from sequential flood and ebb tides from November 2015 through September 2018 and discrete samples from sequential flood and ebb tides from June 2020 through December 2021 across seasons and tidal periods. mg/L as N, milligram per liter as nitrogen; >, greater than, <, less than.

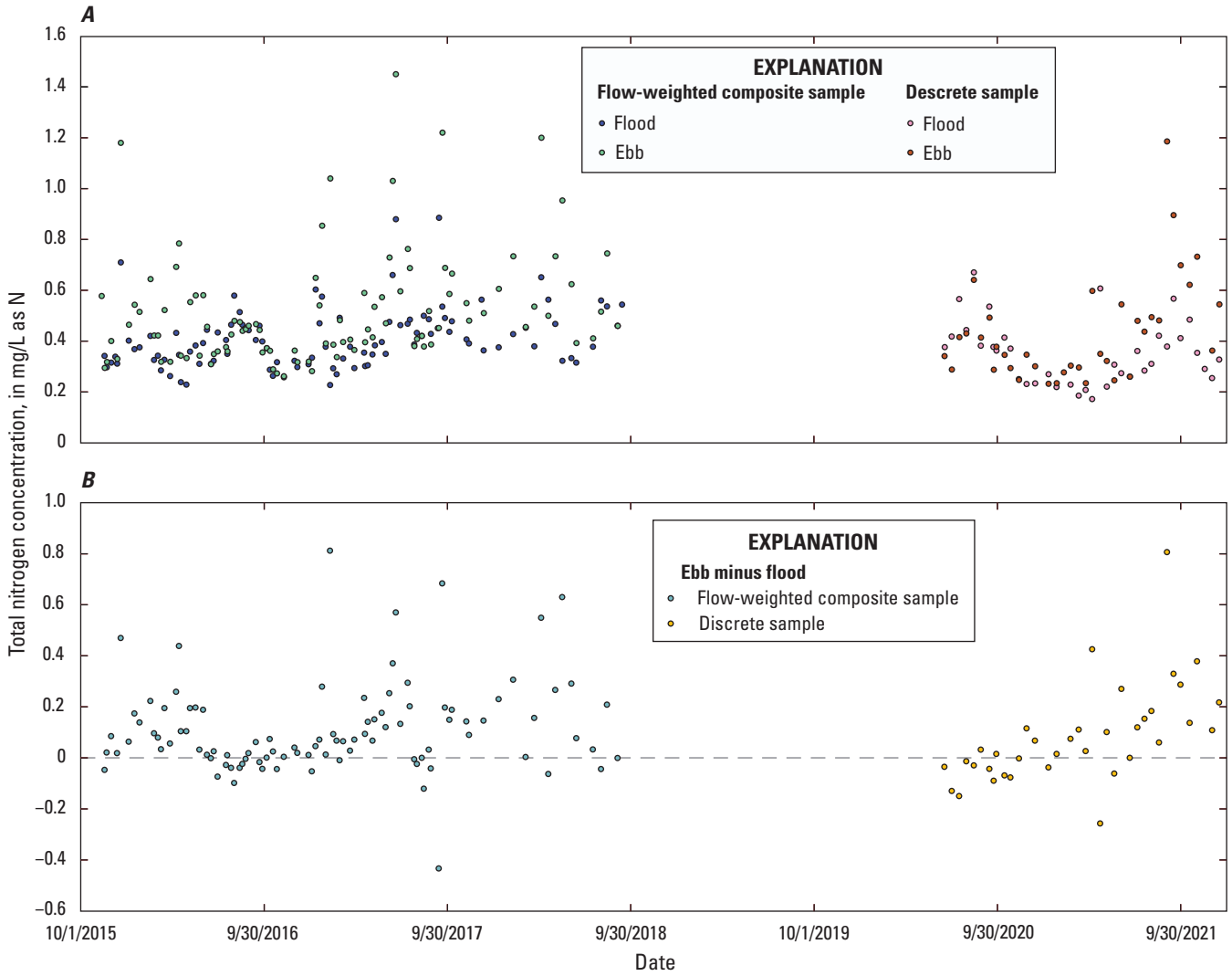

Figure 8. Graphs showing total nitrogen concentrations in the Herring River at Chequessett Neck Road in Wellfleet, Massachusetts, for flow-weighted composite samples from sequential flood and ebb tides from November 2015 through September 2018 and discrete samples from sequential flood and ebb tides from June 2020 through December 2021. *A*, Concentration measurements and *B*, the difference (ebb minus flood) in concentrations. mg/L as N, milligram per liter as nitrogen.

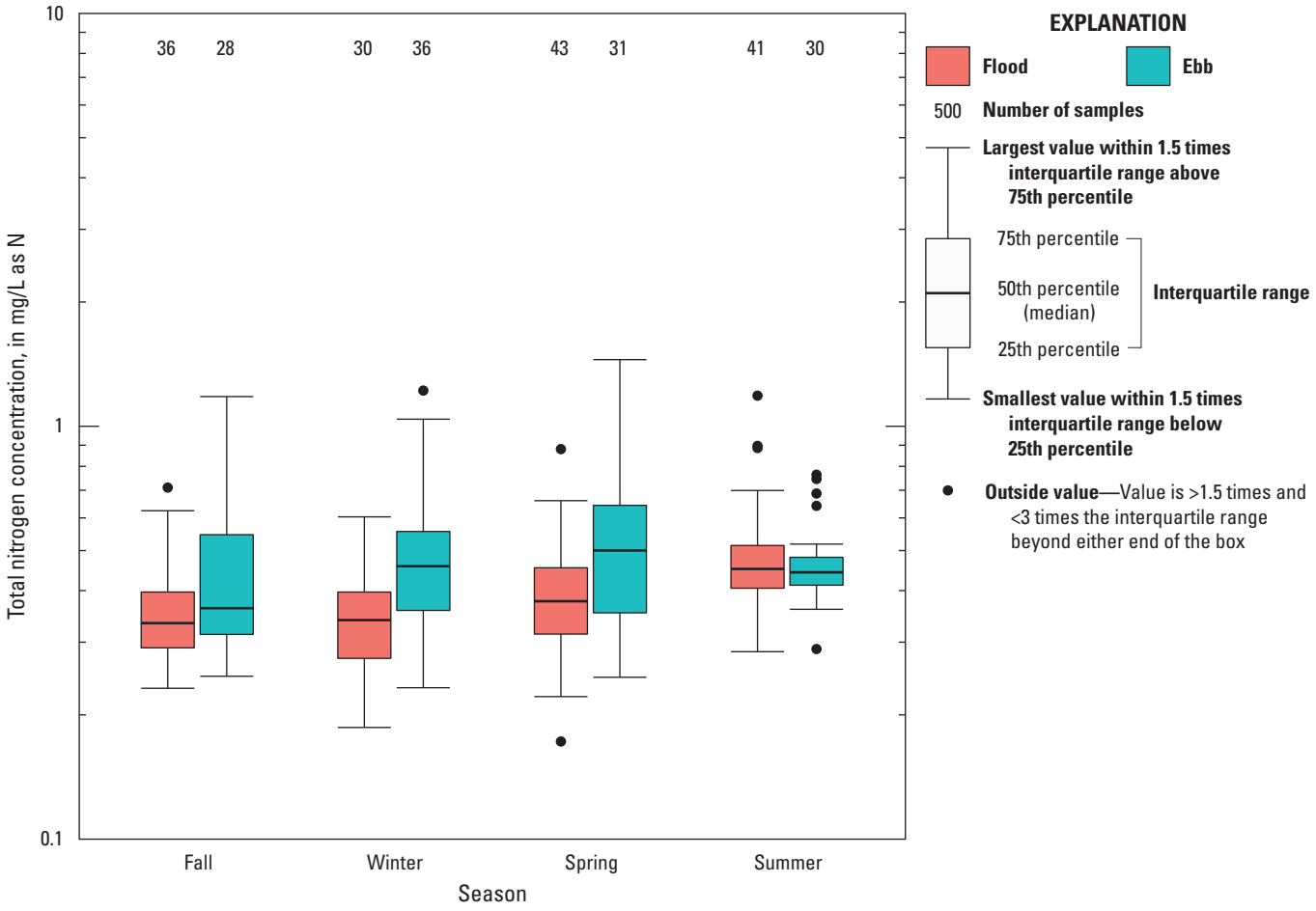

Figure 9. Boxplot showing total nitrogen concentrations in the Herring River at Chequessett Neck Road in Wellfleet, Massachusetts, for flow-weighted composite samples from sequential flood and ebb tides from November 2015 through September 2018 and discrete samples from sequential flood and ebb tides from June 2020 through December 2021 across seasons and tidal periods. mg/L as N, milligram per liter as nitrogen; >, greater than, <, less than.

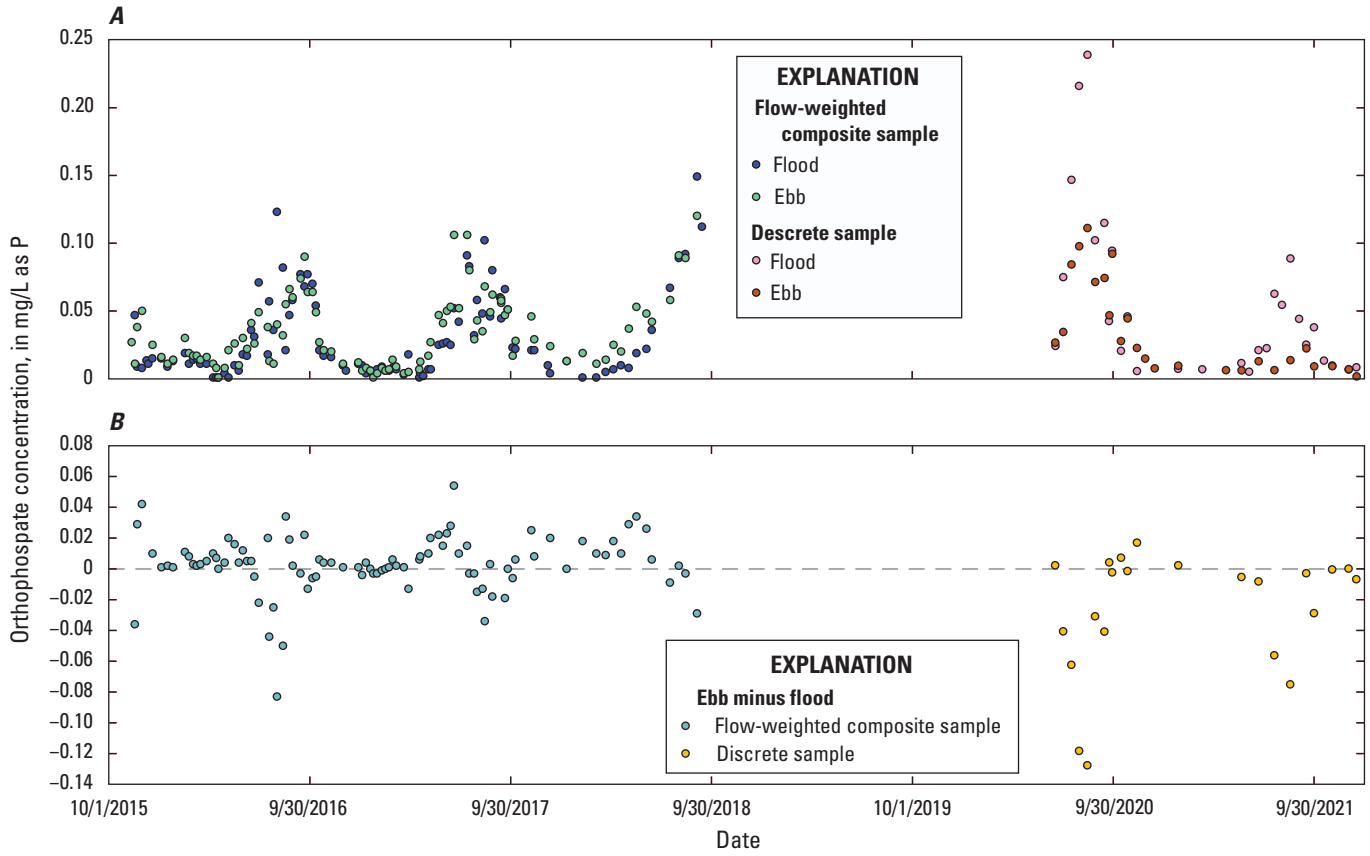

Figure 10. Graphs showing orthophosphate concentrations in the Herring River at Chequessett Neck Road in Wellfleet, Massachusetts, for flow-weighted composite samples from sequential flood and ebb tides from November 2015 through September 2018 and discrete samples from sequential flood and ebb tides from June 2020 through December 2021. *A*, Concentration measurements and *B*, the difference (ebb minus flood) in concentrations. mg/L as P, milligram per liter as phosphorus.

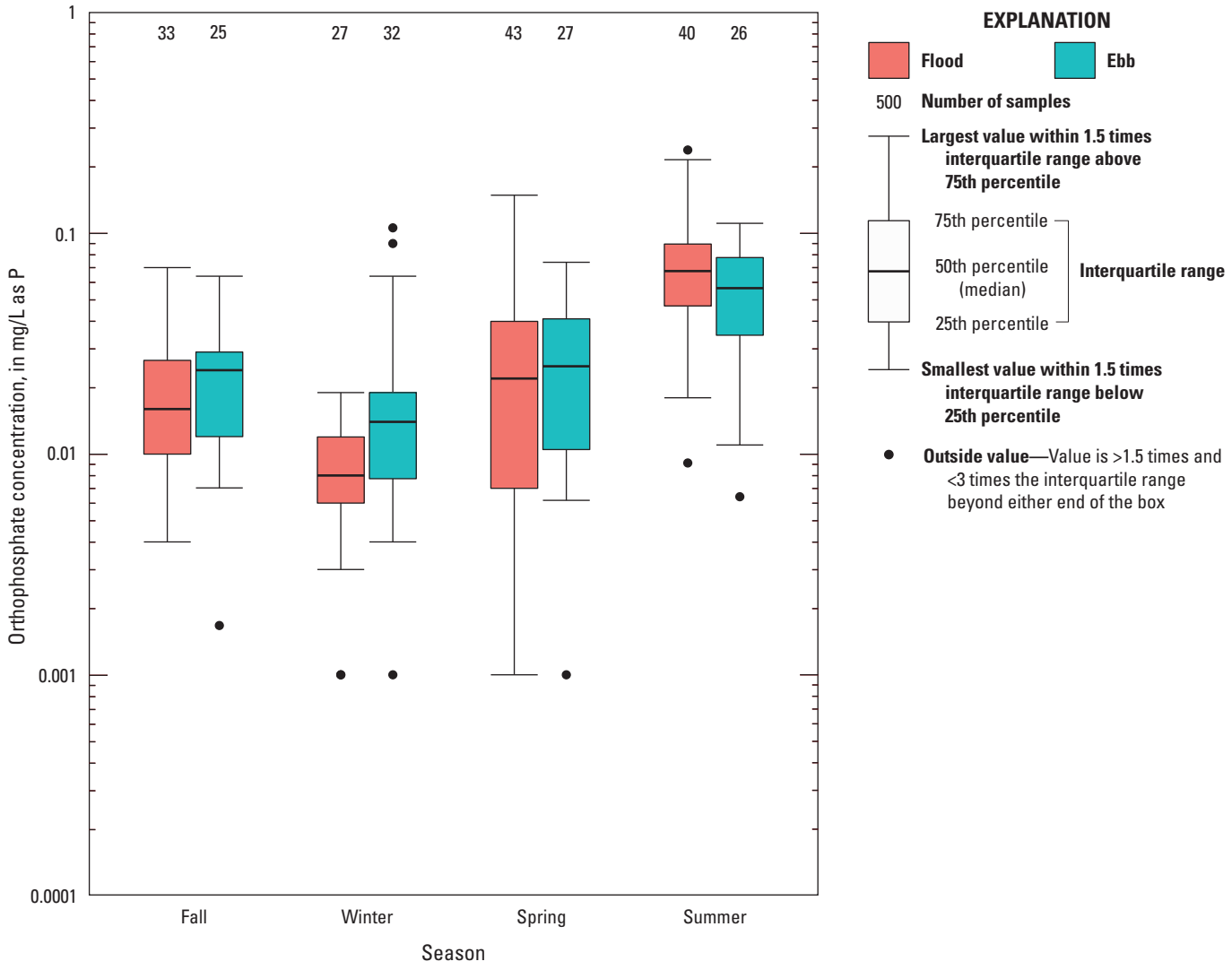

Figure 11. Boxplot showing orthophosphate concentrations in the Herring River at Chequessett Neck Road in Wellfleet, Massachusetts, for flow-weighted composite samples from sequential flood and ebb tides from November 2015 through September 2018 and discrete samples from sequential flood and ebb tides from June 2020 through December 2021 across seasons and tidal periods. mg/L as P, milligram per liter as phosphorus; >, greater than, <, less than.

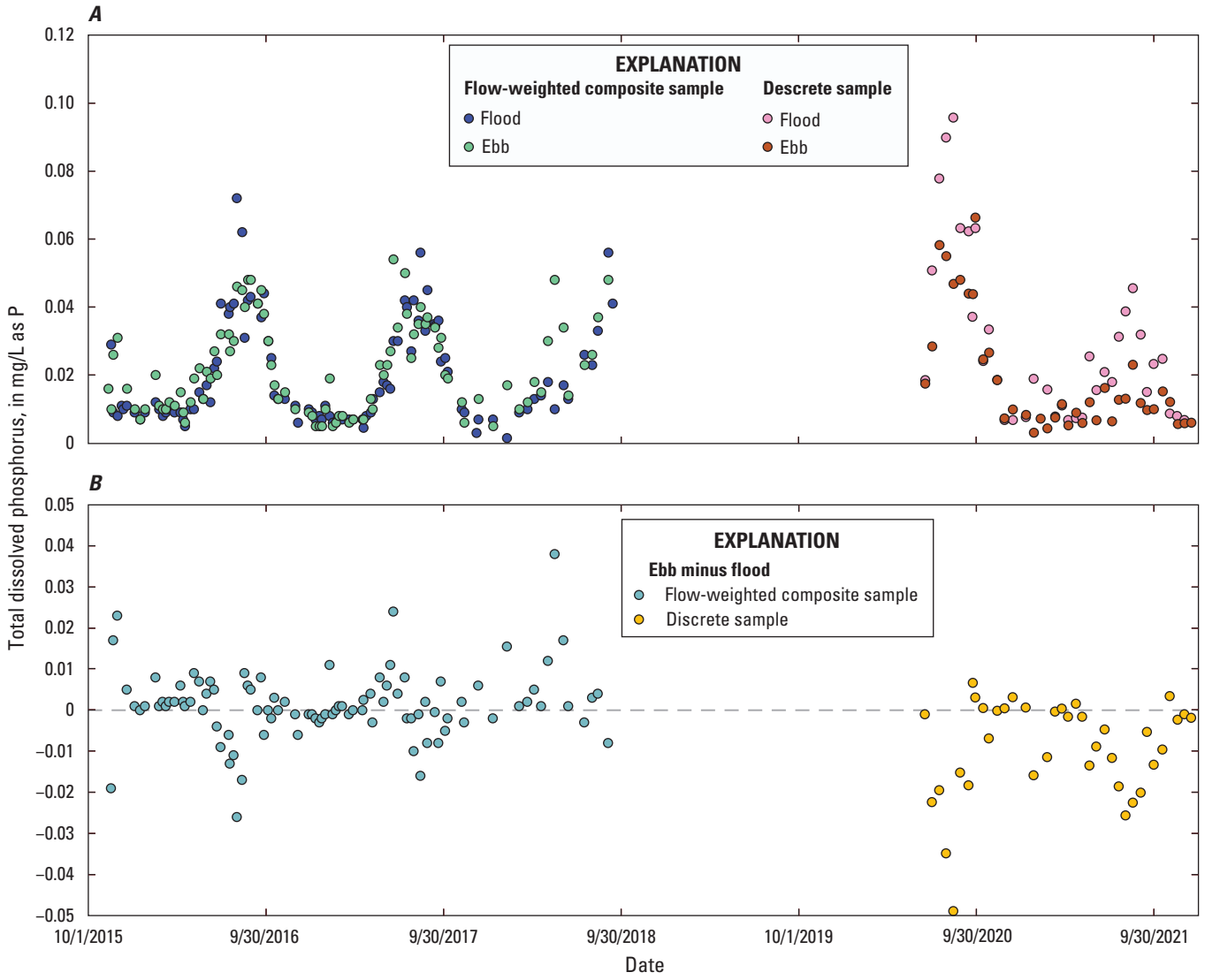

Figure 12. Graphs showing total dissolved phosphorus concentrations in the Herring River at Chequessett Neck Road in Wellfleet, Massachusetts, for flow-weighted composite samples from sequential flood and ebb tides from November 2015 through September 2018 and discrete samples from sequential flood and ebb tides from June 2020 through December 2021. *A*, Concentration measurements and *B*, the difference (ebb minus flood) in concentrations. mg/L as P, milligram per liter as phosphorus.

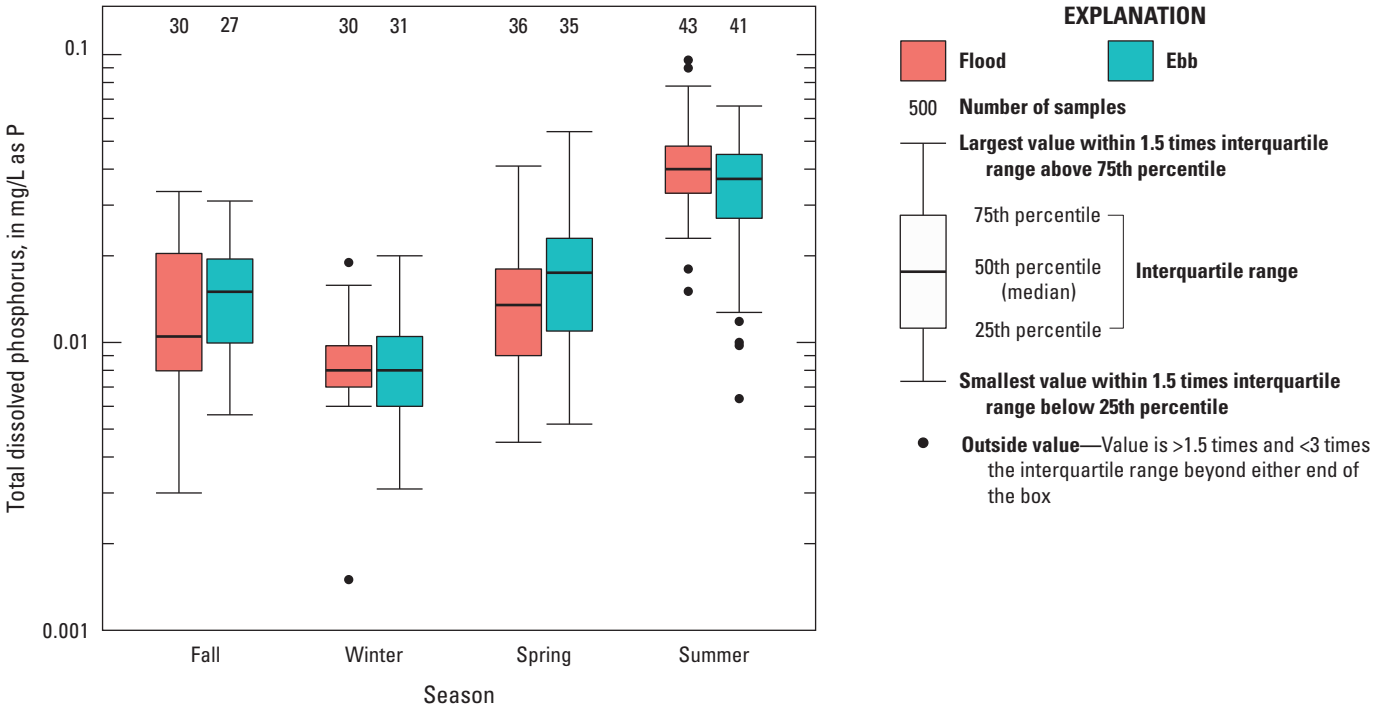

Figure 13. Boxplot showing total dissolved phosphorus concentrations in the Herring River at Chequessett Neck Road in Wellfleet, Massachusetts, for flow-weighted composite samples from sequential flood and ebb tides from November 2015 through September 2018 and discrete samples from sequential flood and ebb tides from June 2020 through December 2021 across seasons and tidal periods. mg/L as P, milligram per liter as phosphorus; >, greater than, <, less than.

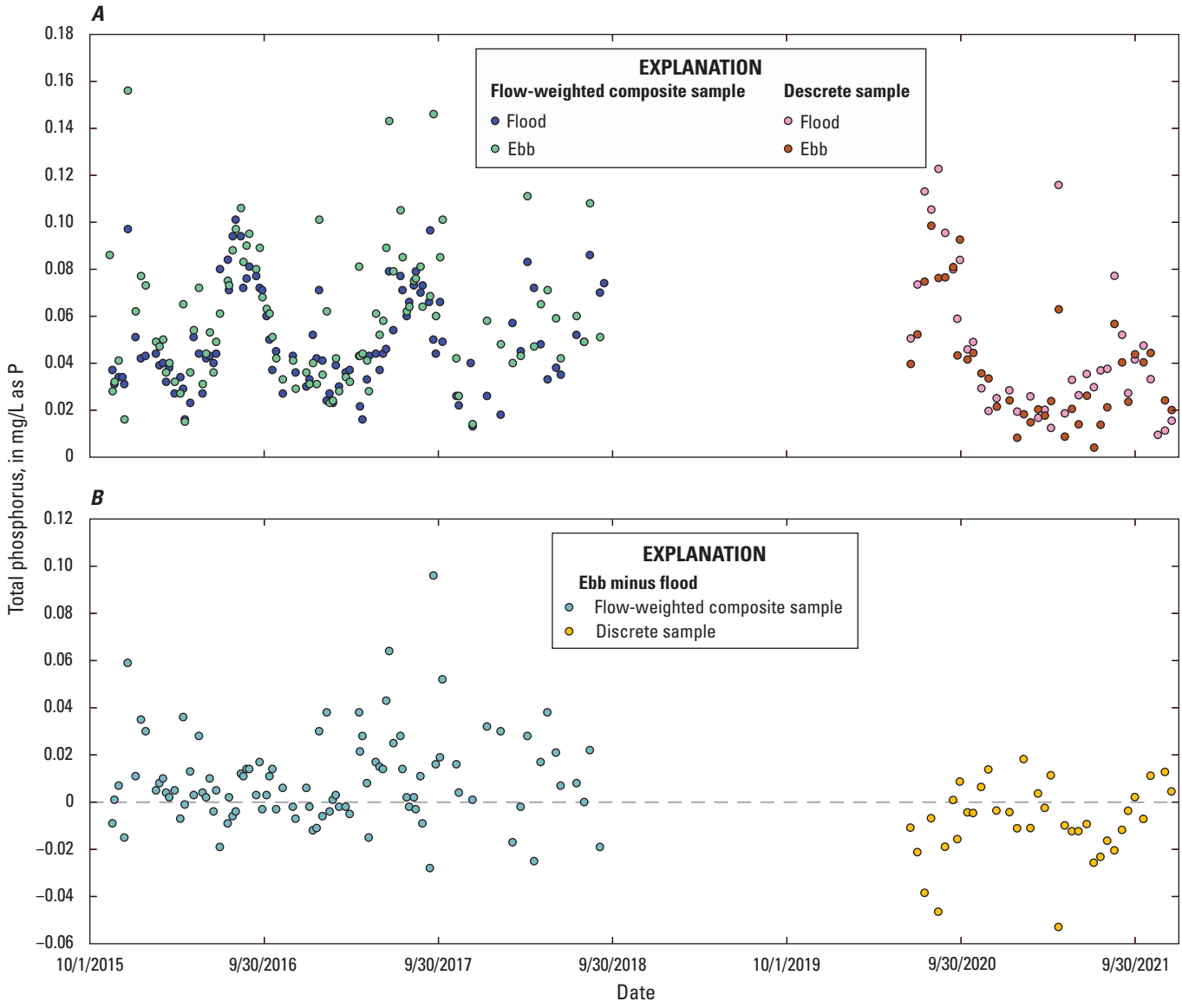

Figure 14. Graphs showing total phosphorus concentrations in the Herring River at Chequessett Neck Road in Wellfleet, Massachusetts, for flow-weighted composite samples from sequential flood and ebb tides from November 2015 through September 2018 and discrete samples from sequential flood and ebb tides from June 2020 through December 2021. *A*, Concentration measurements and *B*, the difference (ebb minus flood) in concentrations. mg/L as P, milligram per liter as phosphorus.

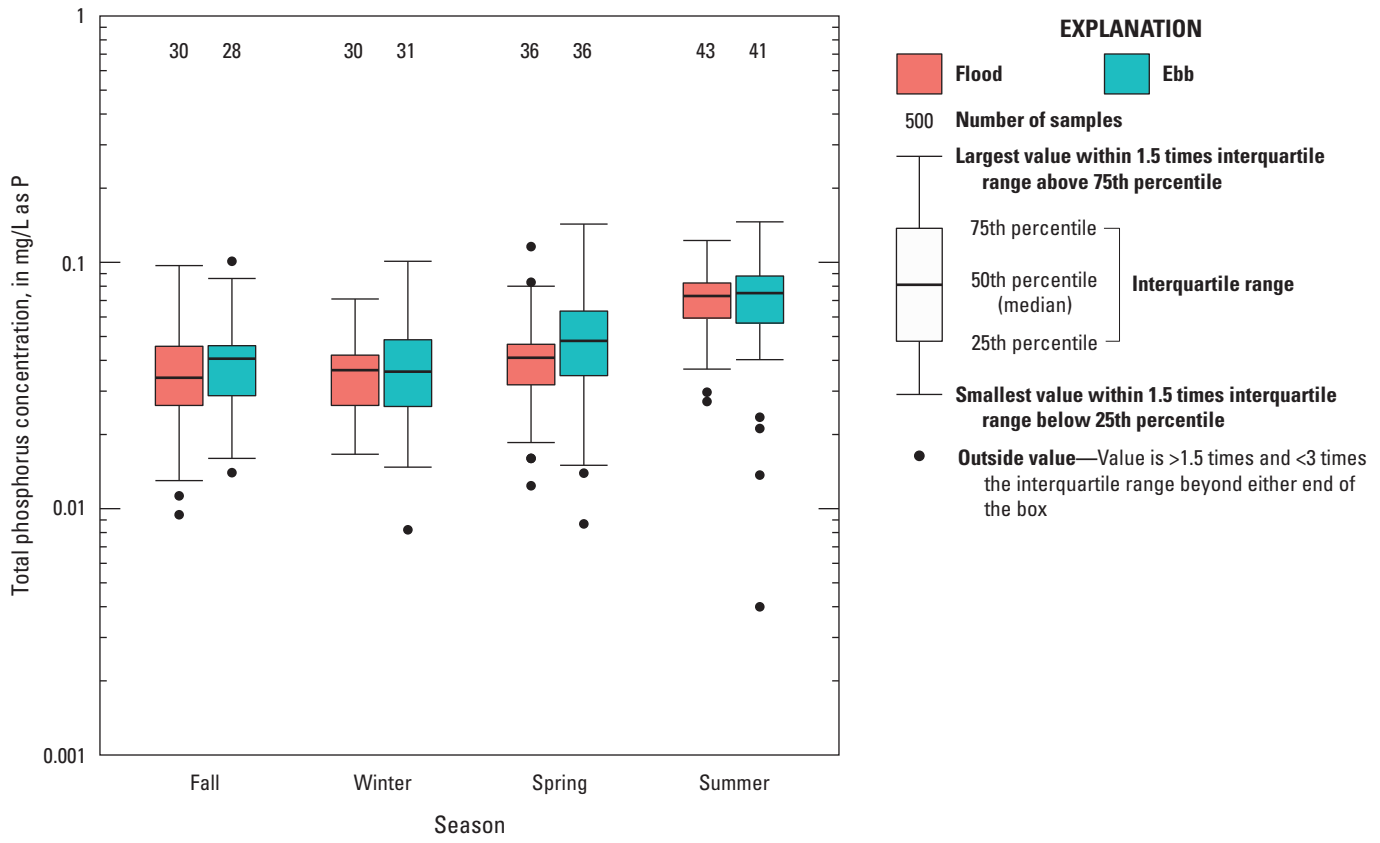

Figure 15. Boxplot showing total phosphorus concentrations in the Herring River at Chequessett Neck Road in Wellfleet, Massachusetts, for flow-weighted composite samples from sequential flood and ebb tides from November 2015 through September 2018 and discrete samples from sequential flood and ebb tides from June 2020 through December 2021 across seasons and tidal periods. mg/L as P, milligram per liter as phosphorus; >, greater than, <, less than.

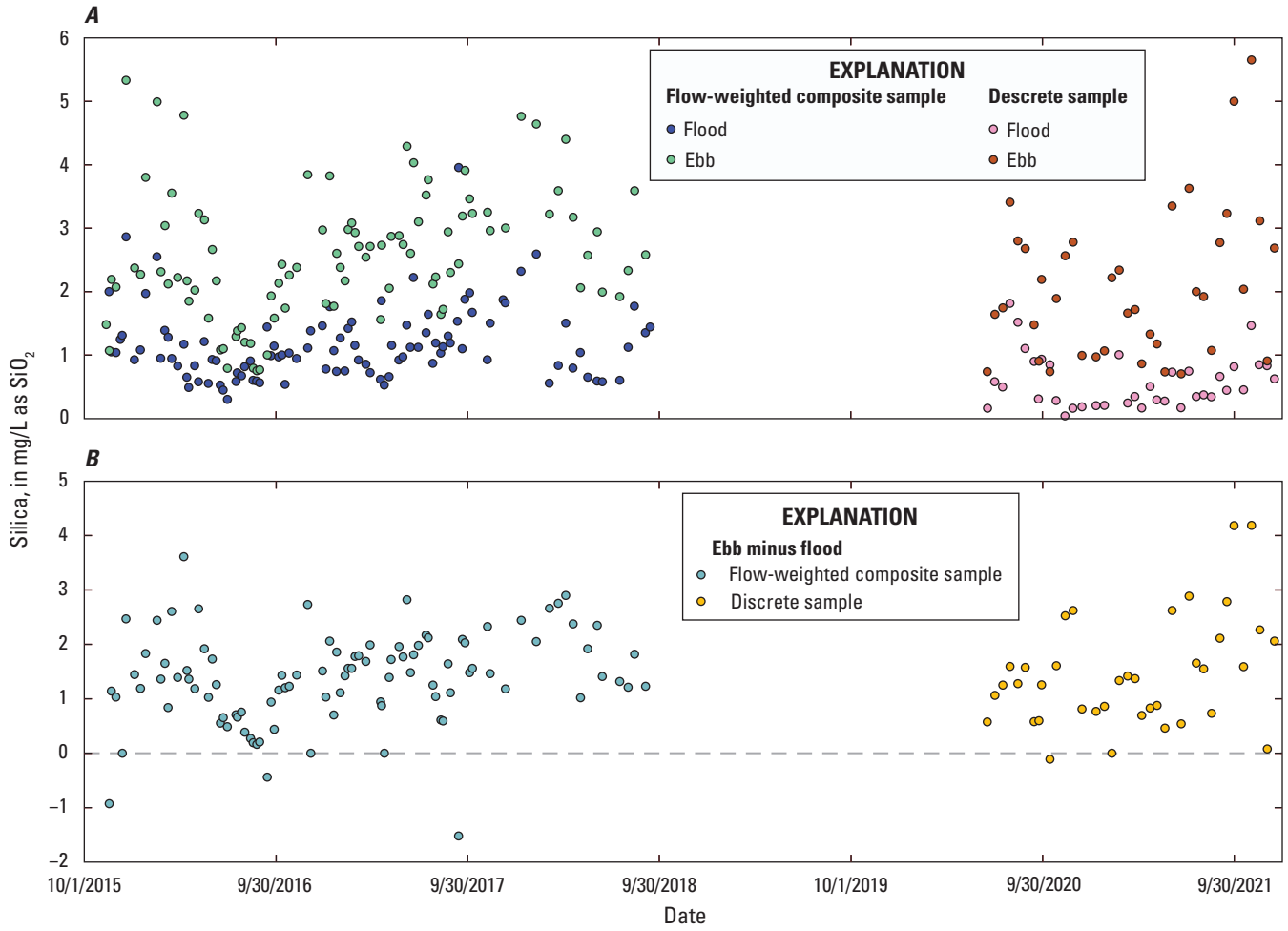

Figure 16. Graphs showing silica concentrations in the Herring River at Chequessett Neck Road in Wellfleet, Massachusetts, for flow-weighted composite samples from sequential flood and ebb tides from November 2015 through September 2018 and discrete samples from sequential flood and ebb tides from June 2020 through December 2021. *A*, Concentration measurements and *B*, the difference (ebb minus flood) in concentrations. mg/L as SiO_2, milligram per liter as silica.

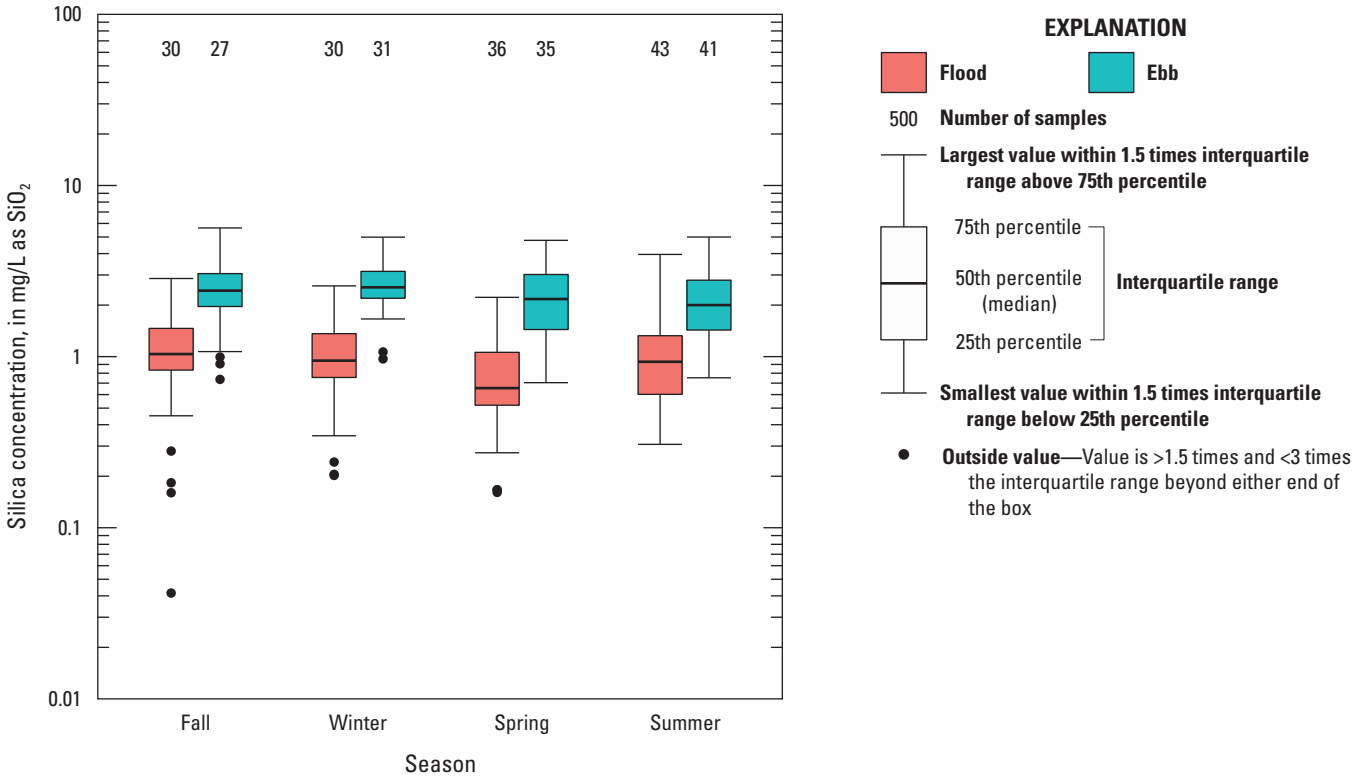

Figure 17. Boxplot showing silica concentrations in the Herring River at Chequessett Neck Road in Wellfleet, Massachusetts, for flow-weighted composite samples from sequential flood and ebb tides from November 2015 through September 2018 and discrete samples from sequential flood and ebb tides from June 2020 through December 2021 across seasons and tidal periods. mg/L as SiO_2, milligram per liter as silica; >, greater than; <, less than.

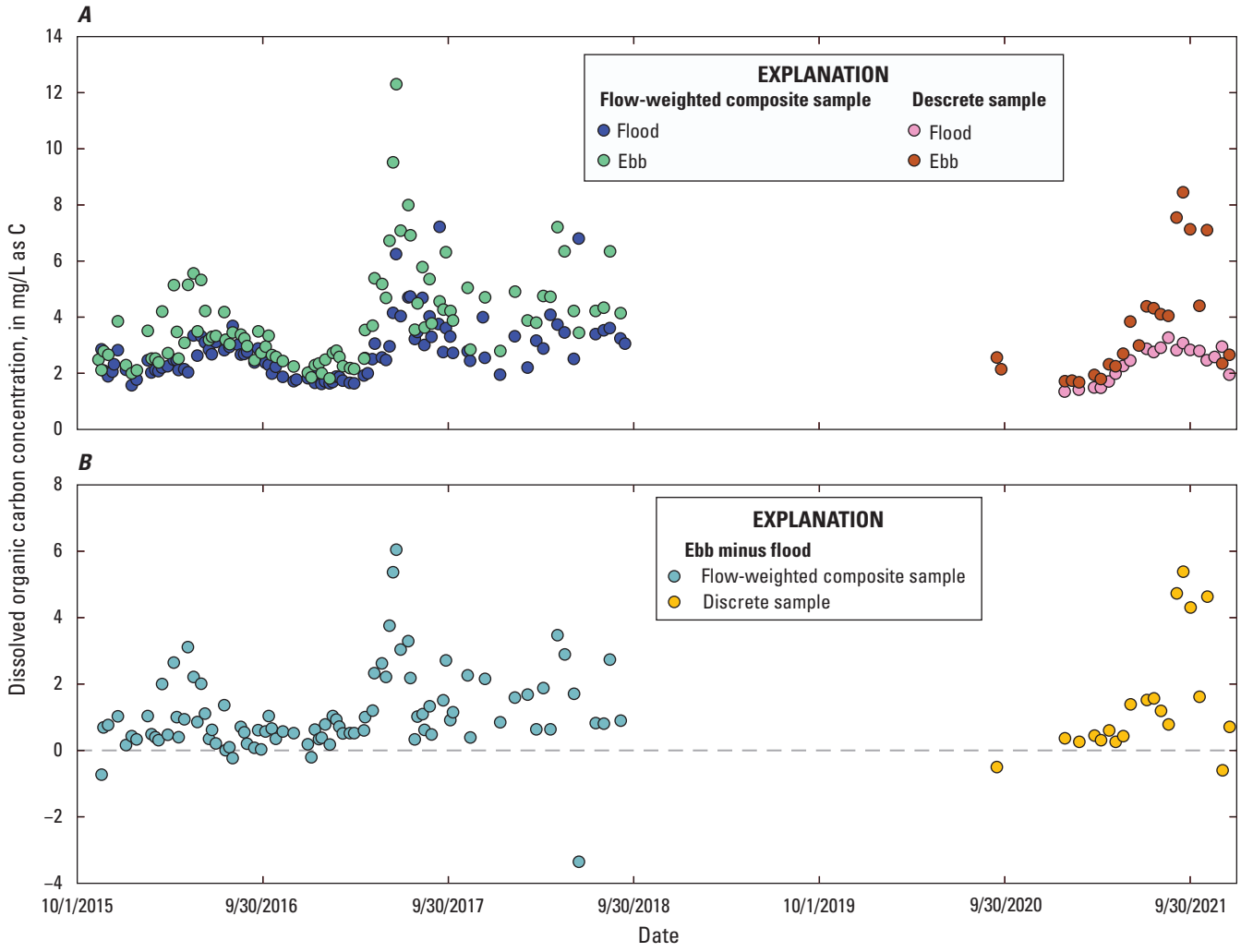

Figure 18. Graphs showing dissolved organic carbon concentrations in the Herring River at Chequessett Neck Road in Wellfleet, Massachusetts, for flow-weighted composite samples from sequential flood and ebb tides from November 2015 through September 2018 and discrete samples from sequential flood and ebb tides from June 2020 through December 2021. *A*, Concentration measurements and *B*, the difference (ebb minus flood) in concentrations. mg/L as C, milligram per liter as carbon.

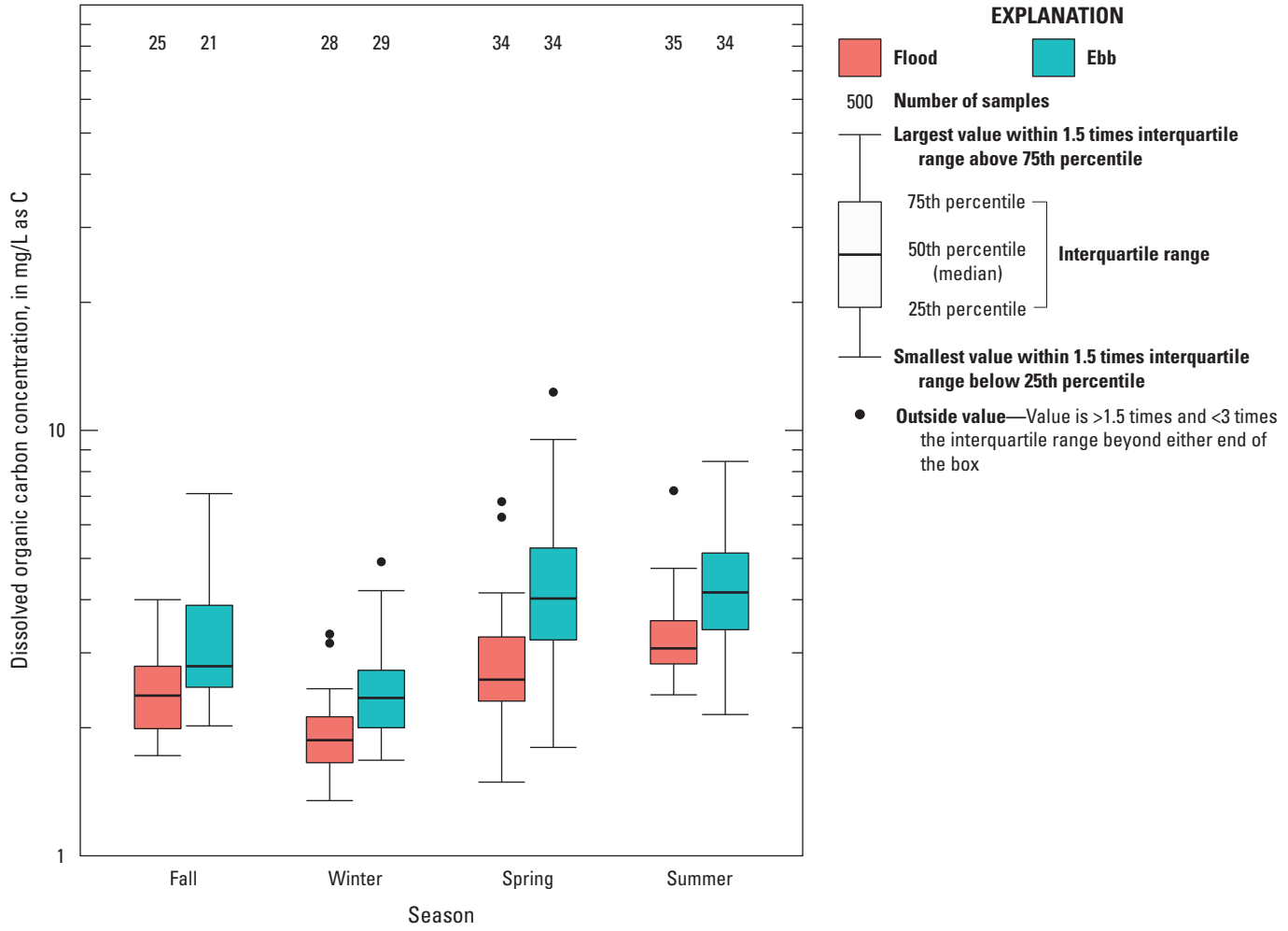

Figure 19. Boxplot showing dissolved organic carbon concentrations in the Herring River at Chequessett Neck Road in Wellfleet, Massachusetts, for flow-weighted composite samples from sequential flood and ebb tides from November 2015 through September 2018 and discrete samples from sequential flood and ebb tides from June 2020 through December 2021 across seasons and tidal periods. mg/L as C, milligram per liter as carbon; >, greater than, <, less than.

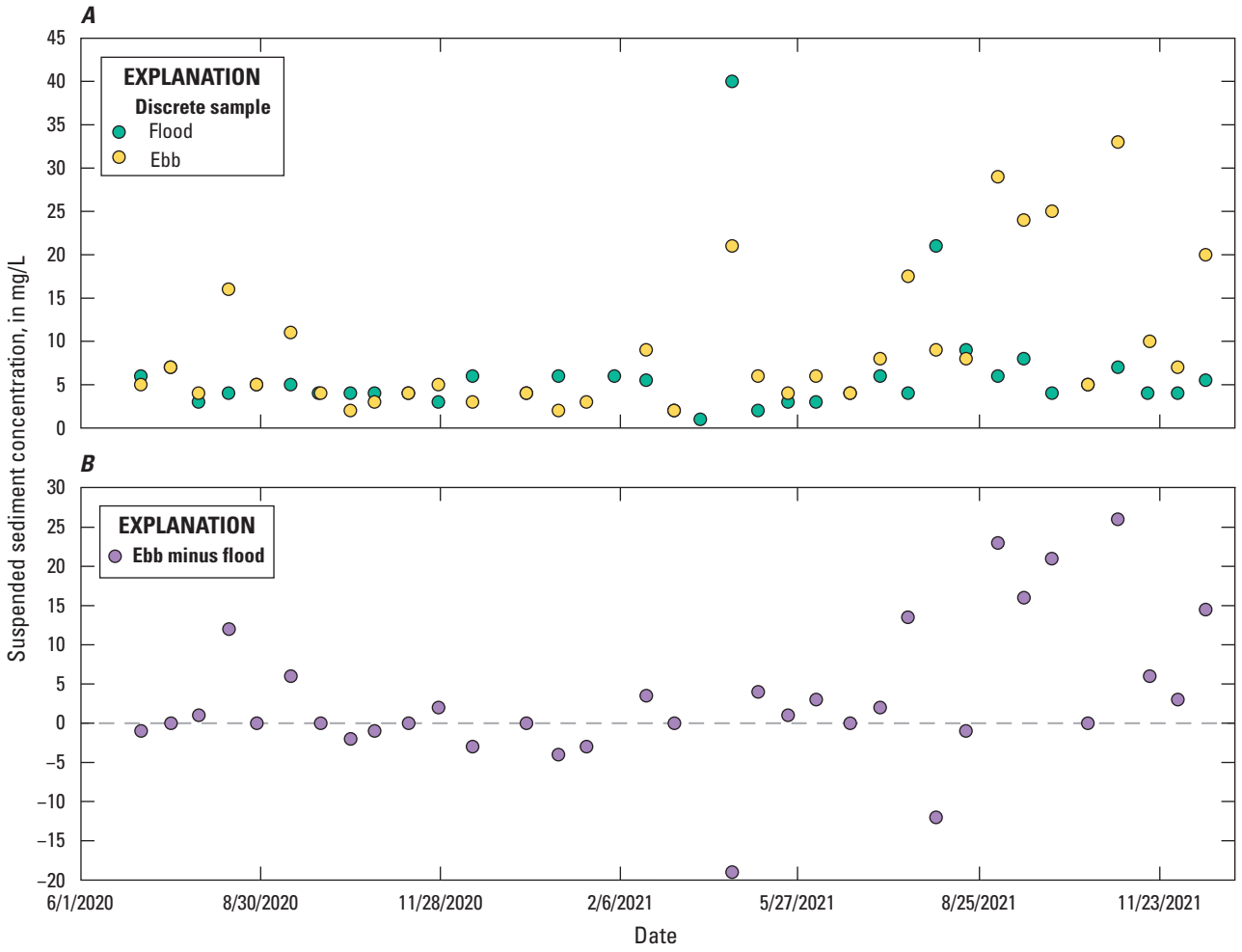

Figure 20. Graphs showing suspended sediment concentrations in the Herring River at Chequessett Neck Road in Wellfleet, Massachusetts, for discrete samples from sequential flood and ebb tides from July 2020 through December 2021. *A*, Concentration measurements and *B*, the difference (ebb minus flood) in concentrations.

Variation in Nutrient Concentration Between Spring, Neap, and Mid Tides

The interquartile ranges and median NO_3 plus NO_2 concentrations were similar for samples collected during spring, neap, and midamplitude tides on flood and ebb tides (fig. 21). The interquartile ranges in NH_4 concentrations were similar, but the median concentrations were higher for samples collected during spring compared with neap tides on flood and ebb tides (fig. 22). The median NH_4 concentrations on the flood tide were 49 percent higher on the spring compared with neap tide, and on the ebb tide, 23 percent higher on the spring compared with neap tide. Samples collected during midamplitude tides were similar to those during spring and neap tides. The interquartile ranges and median TDN and TN concentrations were similar for samples collected during spring, neap, and midamplitude tides (figs. 23 and 24).

The interquartile ranges and median orthophosphate concentrations were similar for samples collected during spring, neap, and midamplitude tides on flood and ebb tides with the exception of higher interquartile range and median concentrations for samples collected on midamplitude ebb tides compared with spring and neap tides (fig. 25). The median orthophosphate concentrations on the ebb tide were 71 and 79 percent higher on the midamplitude compared with spring and neap tides, respectively.

The interquartile ranges and median TDP concentrations were similar for samples collected during spring, neap, and midamplitude tides on flood tides (fig. 26). The interquartile ranges for TDP concentrations were similar for samples collected during spring, neap, and midamplitude tides on ebb tides, but the median concentrations were highest on the midamplitude tides and lowest on the neap tide. On the ebb tide, the TDP concentrations on the midamplitude tide were 92 percent higher than on the neap tide, and the TDP concentrations on the spring tide were 47 percent higher than on the neap tide. On the ebb tide, the TDP concentrations on the spring tide were 31 percent higher than on the neap tide.

The interquartile ranges and median TP concentrations were similar for samples collected during spring, neap, and midamplitude tides on flood and ebb tides with the exception of higher interquartile range and median concentrations for samples collected on midamplitude ebb tides compared with spring and neap tides (fig. 27). The median TP concentrations on the ebb tide were 43 and 45 percent higher on the midamplitude compared with spring and neap tides, respectively.

The interquartile ranges and median SiO_2 concentrations were similar for samples collected during spring, neap, and midamplitude tides on flood and ebb tides with the exception of higher median concentration for samples collected on midamplitude flood tides compared with spring and neap tides (fig. 28). The median SiO_2 concentrations on the flood tide were 43 and 44 percent higher on the midamplitude compared with spring and neap tides, respectively.

The interquartile ranges of DOC concentrations were similar for samples collected during spring, neap, and midamplitude tides on flood and ebb tides (fig. 29). The median DOC concentrations were similar between the spring and midamplitude tides and lower on the neap tide for both flood and ebb tides. The median DOC concentration on the spring tide was 20 percent higher than on the neap tide on the flood tide and 22 percent higher than on the neap tide on the ebb tide.

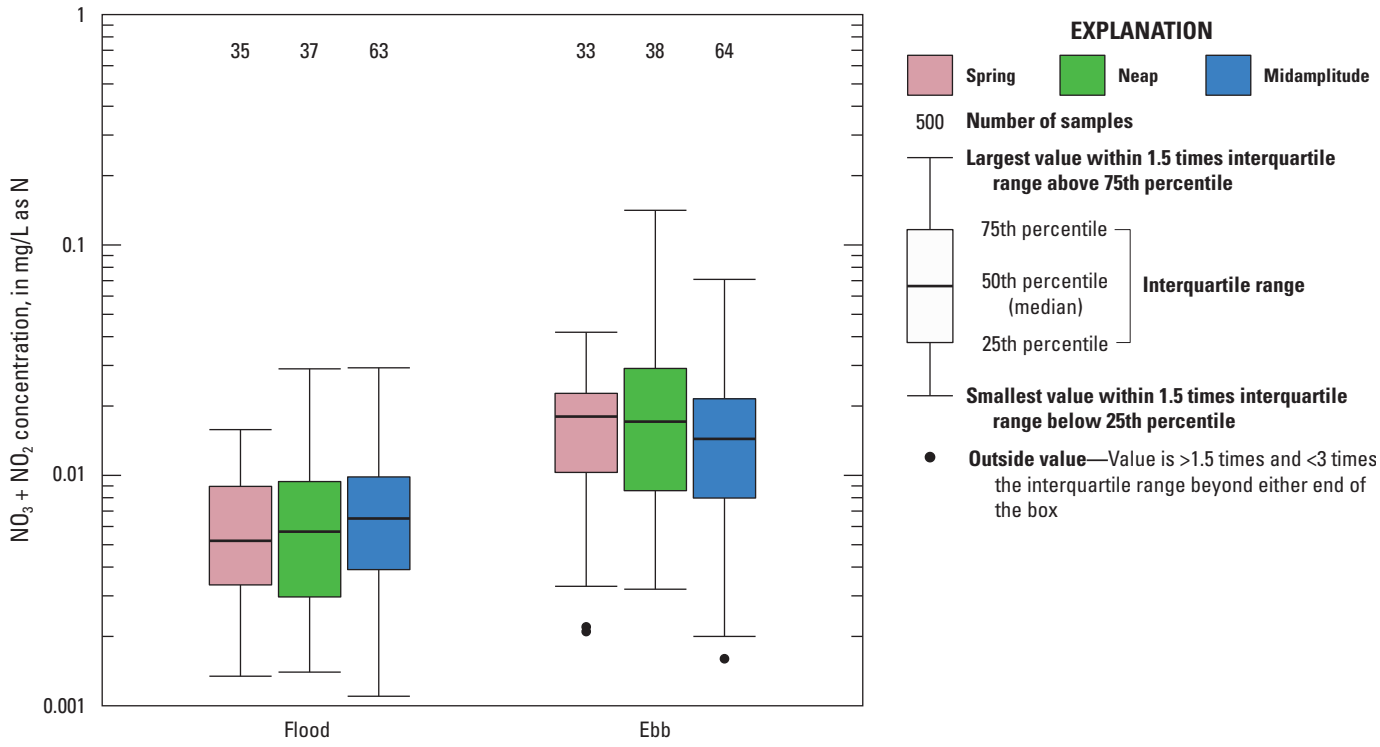

Figure 21. Boxplot showing nitrate plus nitrite concentrations on spring, neap, and midamplitude tides for flood and ebb tides in the Herring River at Chequessett Neck Road in Wellfleet, Massachusetts, for flow-weighted composite samples from sequential flood and ebb tides from November 2015 through September 2018 and discrete samples from sequential flood and ebb tides from June 2020 through December 2021. mg/L as N, milligram per liter as nitrogen; >, greater than, <, less than.

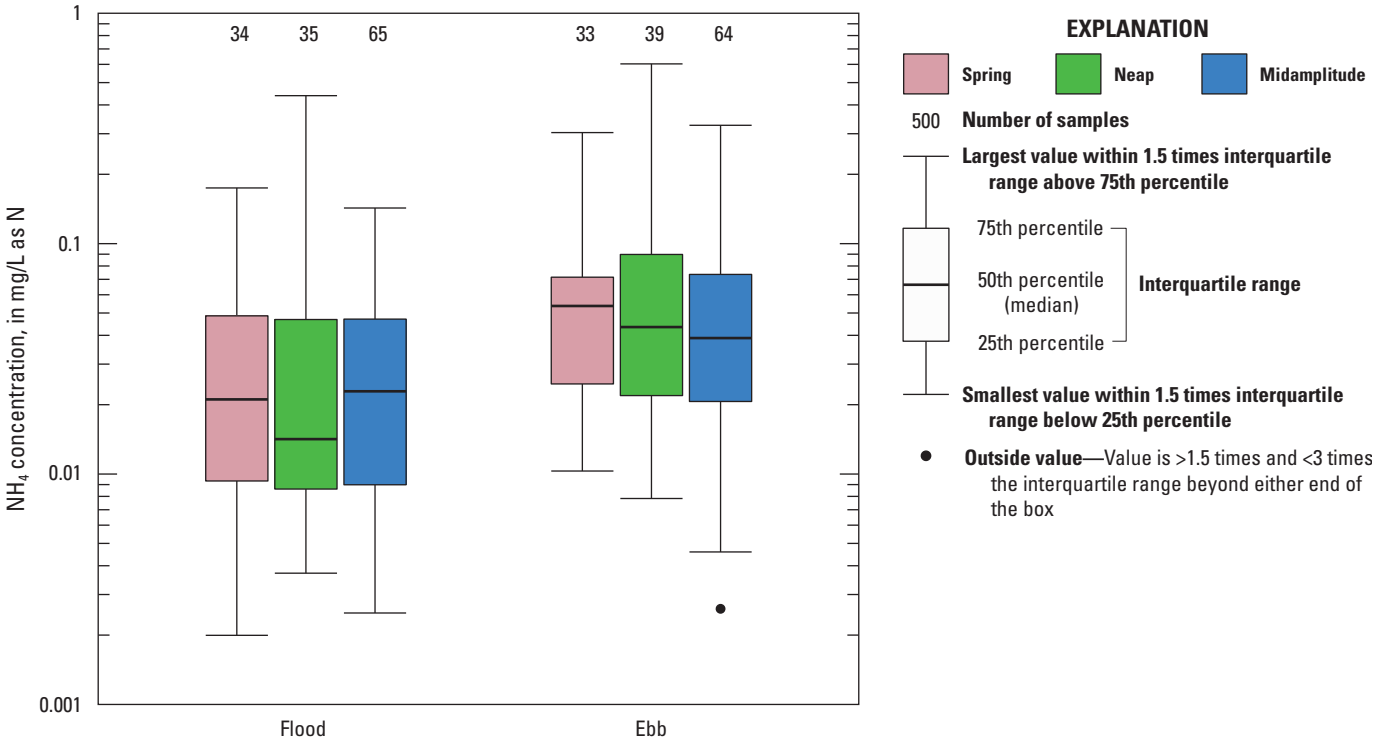

Figure 22. Boxplot showing ammonium concentrations on spring, neap, and midamplitude tides for flood and ebb tides in the Herring River at Chequessett Neck Road in Wellfleet, Massachusetts, for flow-weighted composite samples from sequential flood and ebb tides from November 2015 through September 2018 and discrete samples from sequential flood and ebb tides from June 2020 through December 2021. mg/L as N, milligram per liter as nitrogen; >, greater than, <, less than.

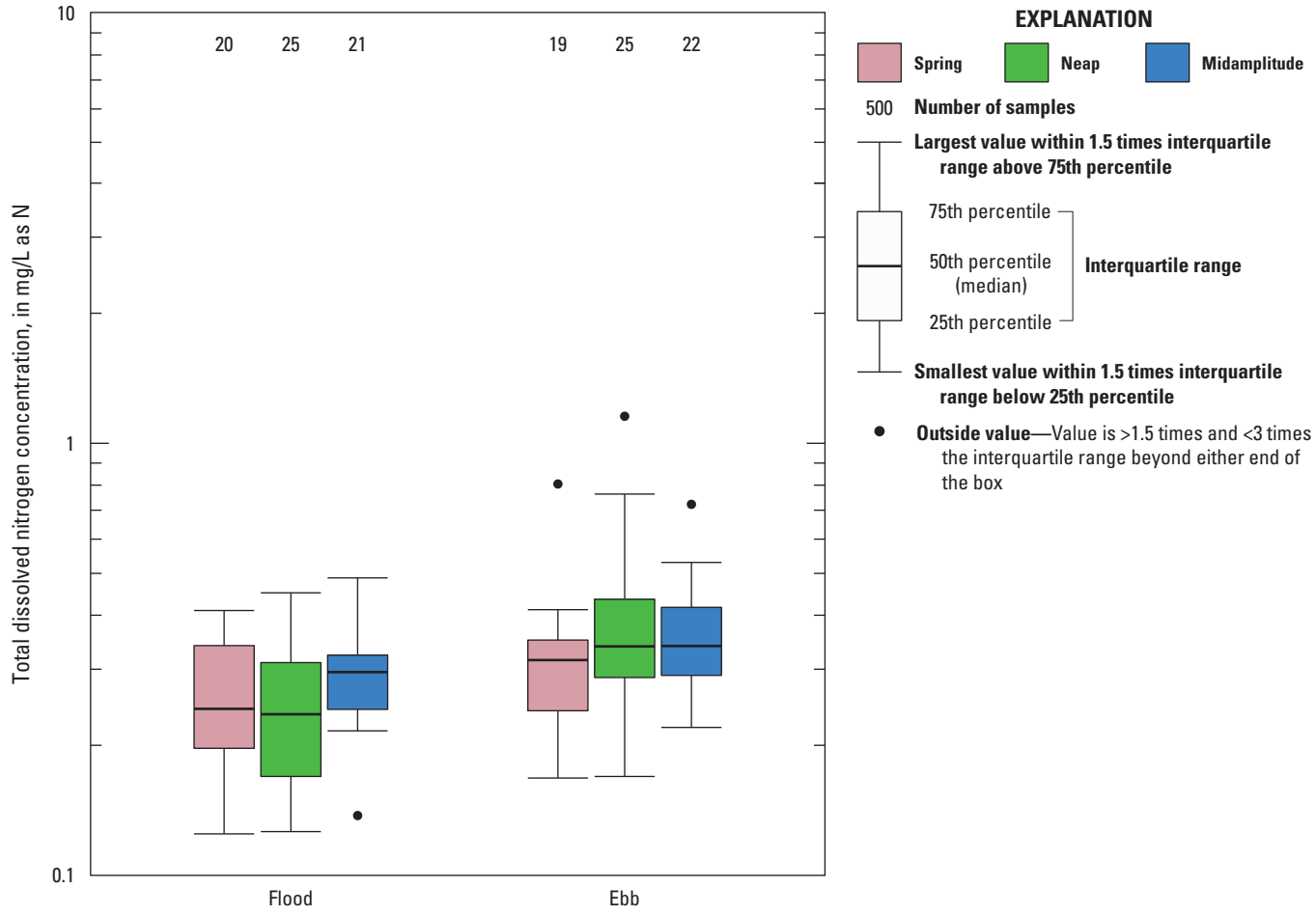

Figure 23. Boxplot showing total dissolved nitrogen concentrations on spring, neap, and midamplitude tides for flood and ebb tides in the Herring River at Chequessett Neck Road in Wellfleet, Massachusetts, for flow-weighted composite samples from sequential flood and ebb tides from October 2017 through September 2018 and discrete samples from sequential flood and ebb tides from June 2020 through December 2021. mg/L as N, milligram per liter as nitrogen; >, greater than, <, less than.

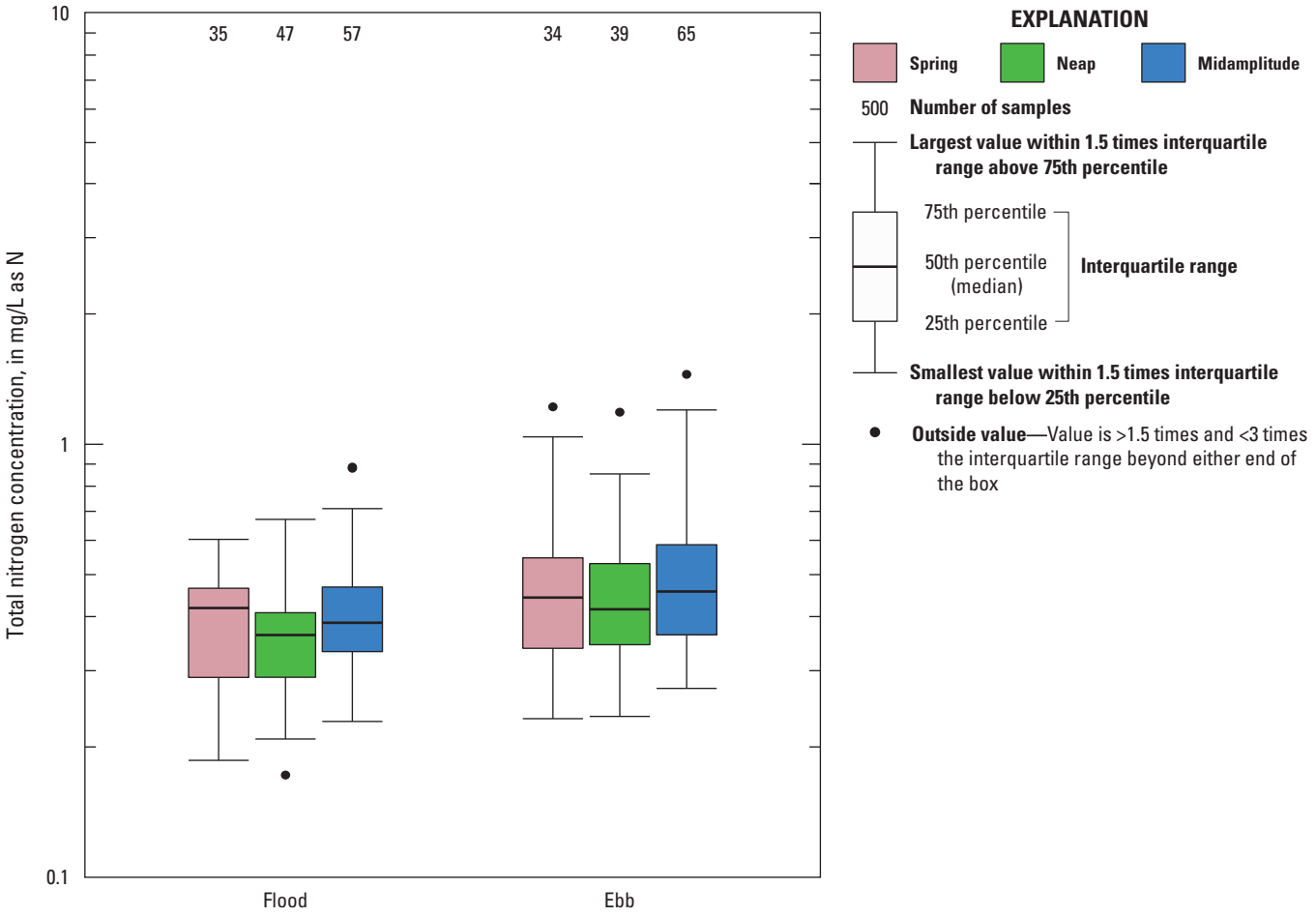

Figure 24. Boxplot showing total nitrogen concentrations on spring, neap, and midamplitude tides for flood and ebb tides in the Herring River at Chequessett Neck Road in Wellfleet, Massachusetts, for flow-weighted composite samples from sequential flood and ebb tides from November 2015 through September 2018 and discrete samples from sequential flood and ebb tides from June 2020 through December 2021. mg/L as N, milligram per liter as nitrogen; >, greater than, <, less than.

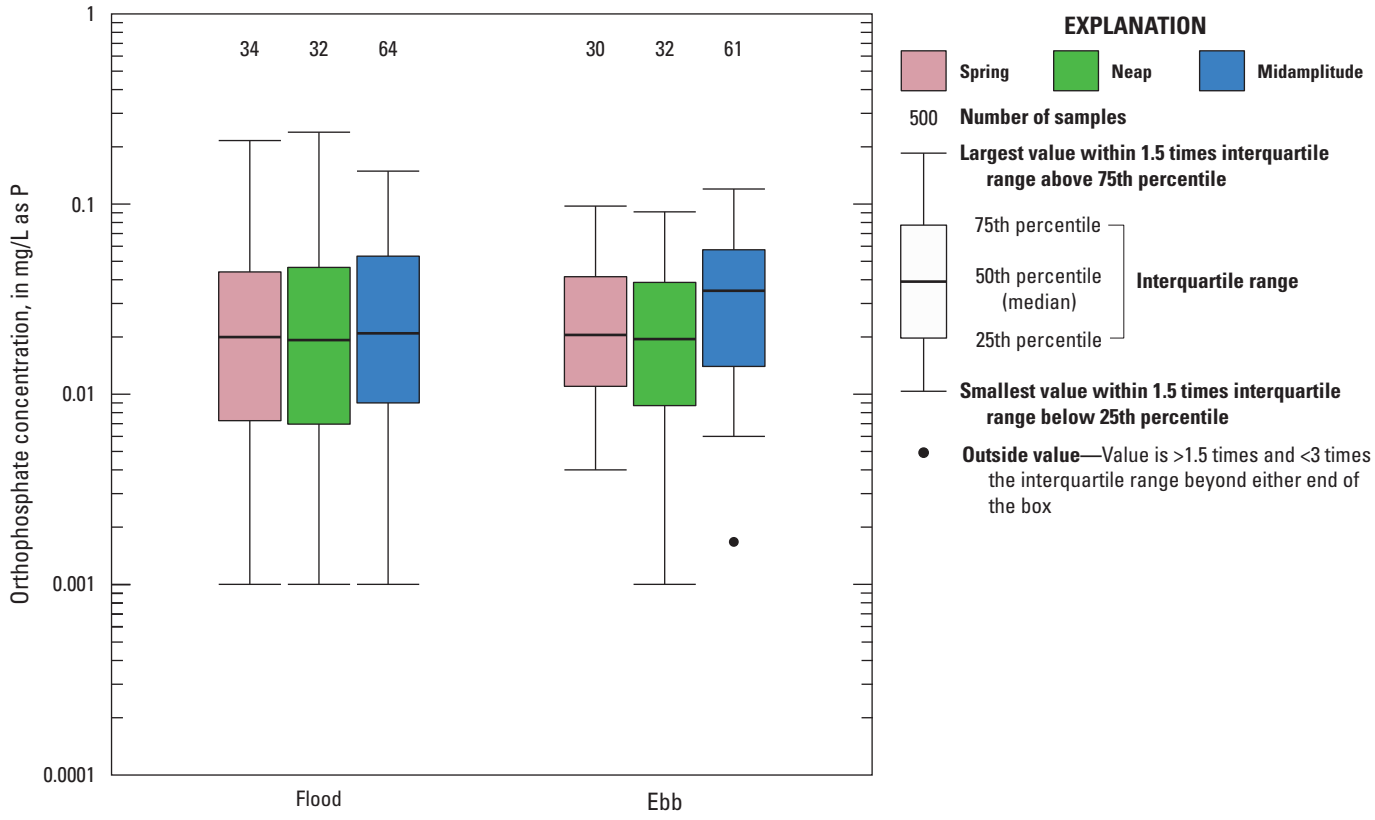

Figure 25. Boxplot showing orthophosphate concentrations on spring, neap, and midamplitude tides for flood and ebb tides in the Herring River at Chequessett Neck Road in Wellfleet, Massachusetts, for flow-weighted composite samples from sequential flood and ebb tides from November 2015 through September 2018 and discrete samples from sequential flood and ebb tides from June 2020 through December 2021. mg/L as P, milligram per liter as phosphorus; >, greater than, <, less than.

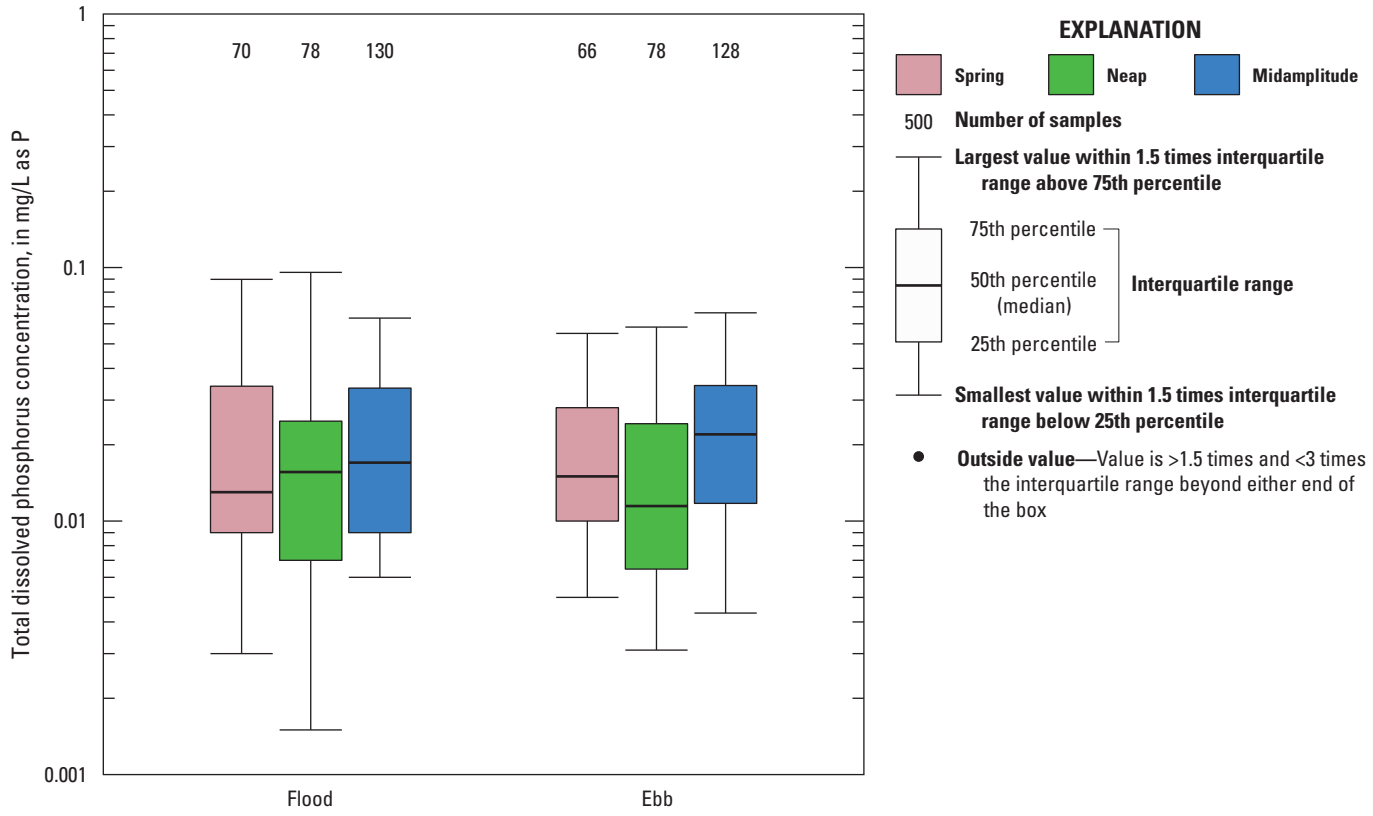

Figure 26. Boxplot showing total dissolved phosphorus concentrations on spring, neap, and midamplitude tides for flood and ebb tides in the Herring River at Chequessett Neck Road in Wellfleet, Massachusetts, for flow-weighted composite samples from sequential flood and ebb tides, November 2015 through September 2018 and discrete samples from sequential flood and ebb tides, June 2020 through December 2021. mg/L as P, milligram per liter as phosphorus; >, greater than, <, less than.

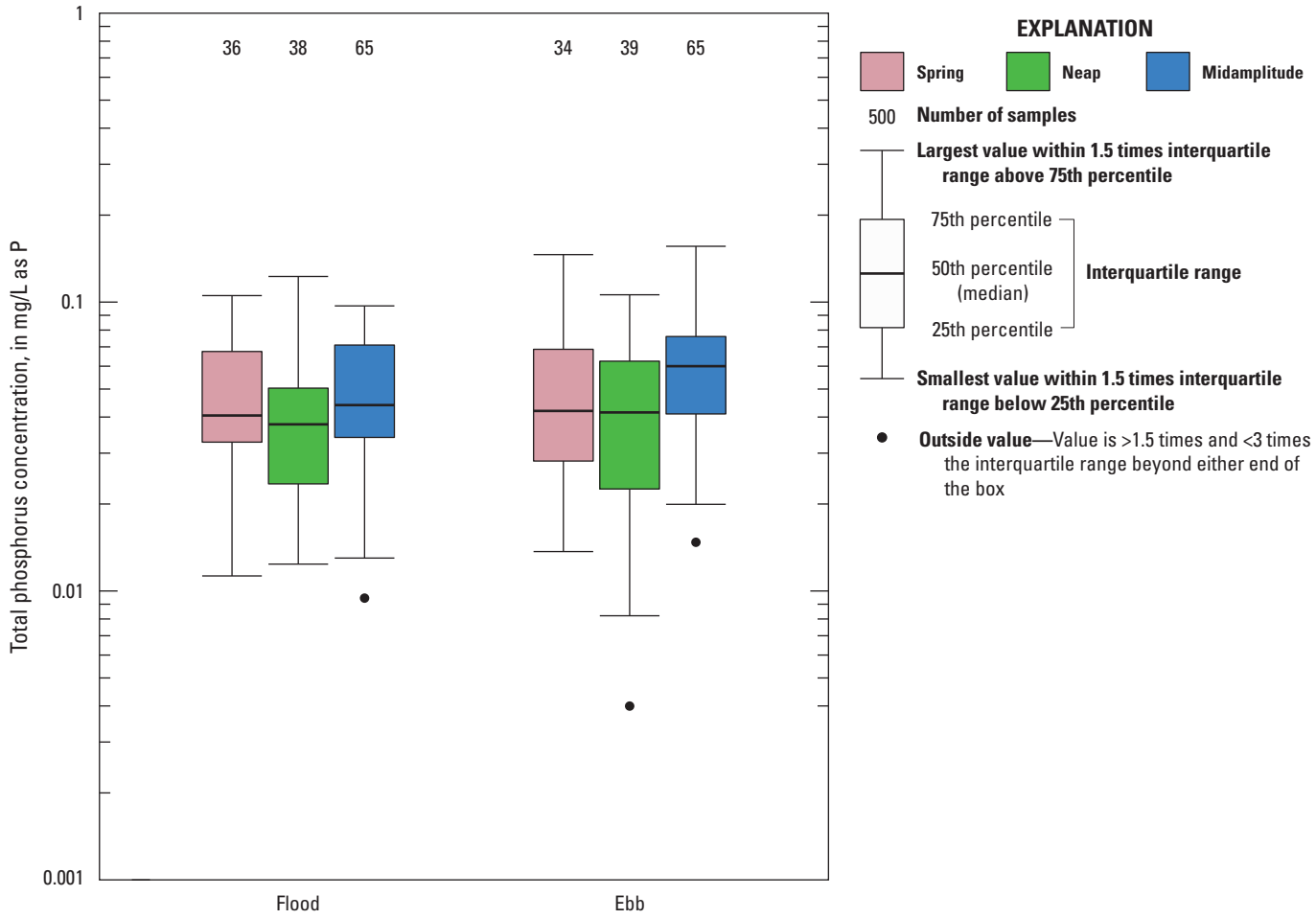

Figure 27. Boxplot showing total phosphorus concentrations on spring, neap, and midamplitude tides for flood and ebb tides in the Herring River at Chequessett Neck Road in Wellfleet, Massachusetts, for flow-weighted composite samples from sequential flood and ebb tides from November 2015 through September 2018 and discrete samples from sequential flood and ebb tides from June 2020 through December 2021. mg/L as P, milligram per liter as phosphorus; >, greater than, <, less than.

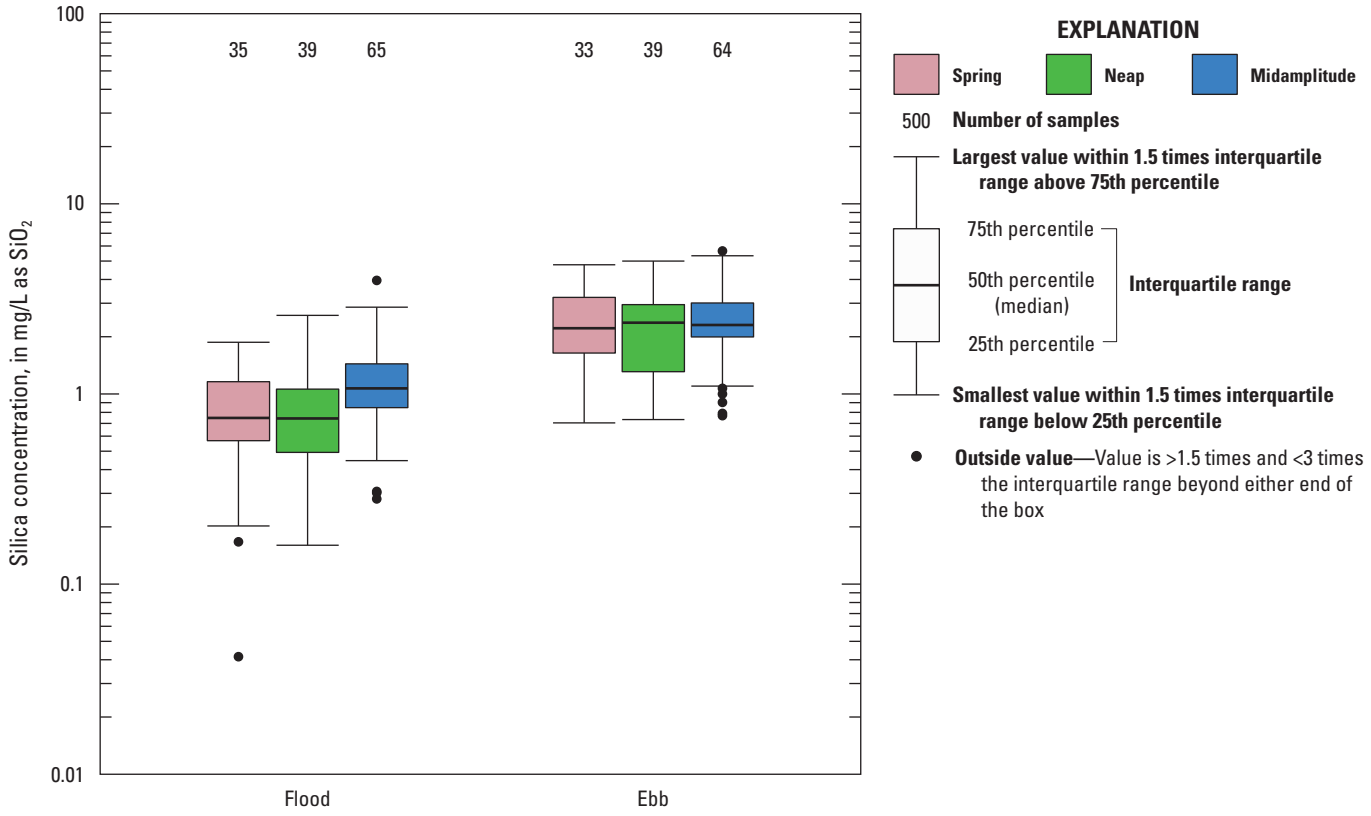

Figure 28. Boxplot showing silica concentrations on spring, neap, and midamplitude tides for flood and ebb tides in the Herring River at Chequessett Neck Road in Wellfleet, Massachusetts, for flow-weighted composite samples from sequential flood and ebb tides from November 2015 through September 2018 and discrete samples from sequential flood and ebb tides from June 2020 through December 2021. mg/L as SiO_2, milligram per liter as silica; >, greater than, <, less than.

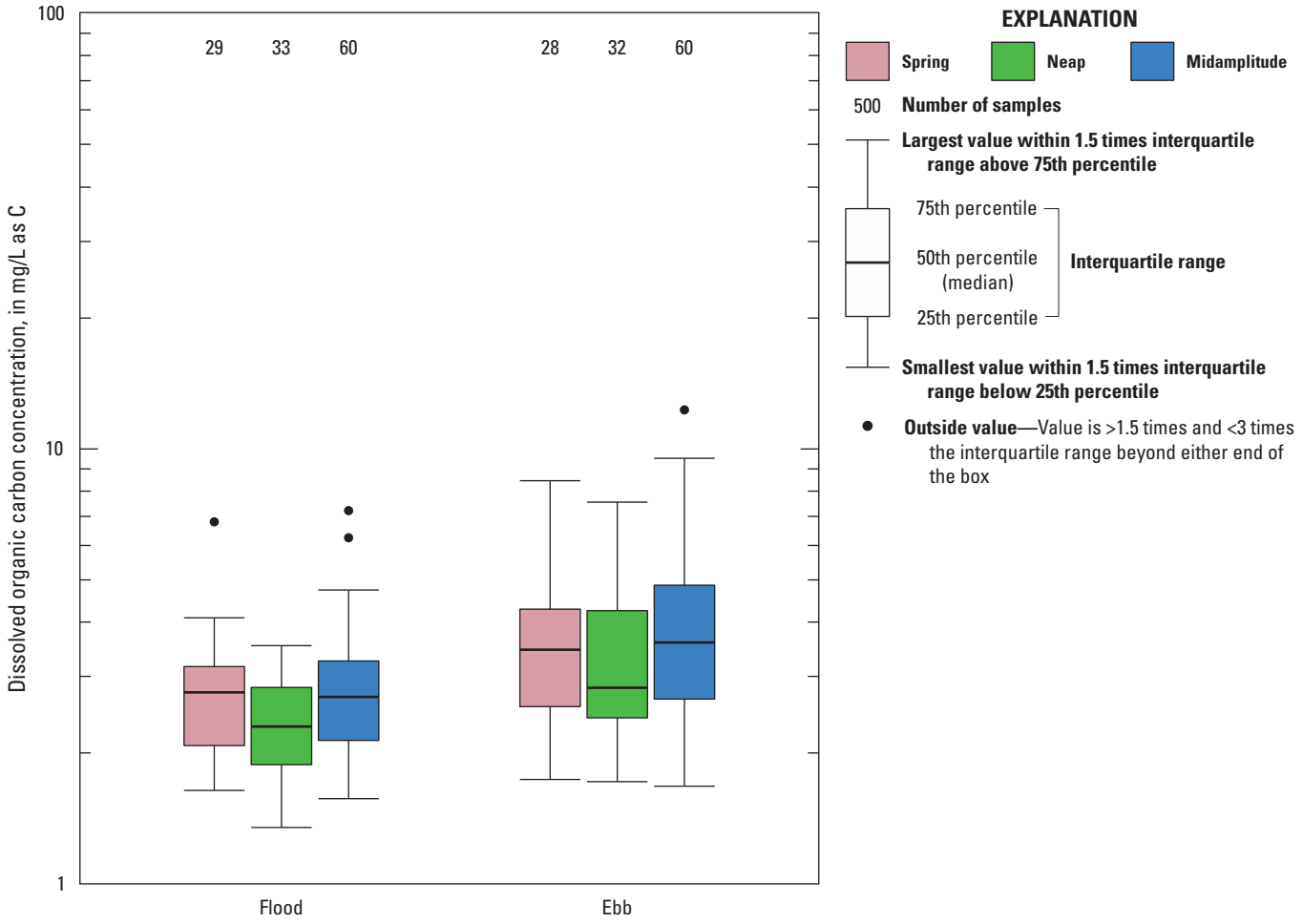

Figure 29. Boxplot showing dissolved organic carbon concentrations on spring, neap, and midamplitude tides for flood and ebb tides in the Herring River at Chequessett Neck Road in Wellfleet, Massachusetts, for flow-weighted composite samples from sequential flood and ebb tides from November 2015 through September 2018 and discrete samples from sequential flood and ebb tides from September 2020 through December 2021. mg/L as C, milligram per liter as carbon; >, greater than, <, less than.

Nutrient Export

In the previous study of Huntington and others (2021), nutrient export from the Herring River watershed at the dike at Chequessett Neck Road was estimated for each ebb tide where concentration and discharge data were available from November 2015 through September 2017. Nutrient export (fluxes) was estimated based on the flow-weighted average concentrations and the total discharge during ebb tides. Discharge was not measured in the current [2023] study, therefore comparable estimates of nutrient export were not possible. It would be possible to estimate monthly nutrient export (fluxes) during the record where nutrient concentration data are available (November 2015 through September 2018 and June 2020 through December 2021) using a different method. Monthly runoff estimates could be calculated using the Thornthwaite water balance model (McCabe and Markstrom, 2007) with input data accessible from gridMET (Abatzoglou, 2013). These runoff estimates for this period are also available in Huntington (2023). Average monthly nutrient concentrations could be calculated by averaging the measurements during each month using the data available in NWIS (U.S. Geological Survey, 2022). Monthly nutrient export could be estimated by multiplying estimated runoff by concentration.

Correlations Between Monthly Average Nutrient Concentrations on the Ebb Tide and Corresponding Monthly Average Environmental Variables

Monthly average NO_3 plus NO_2, NH_4, TN, and SiO_2 concentrations were positively correlated ($p<0.01$) with monthly average precipitation (table 3). These positive correlations could be explained by increases in leaching of nutrients from aboveground organic materials and soils by convective mass flow that typically increases with increasing precipitation volume and intensity (Ballard and others, 2019; Winter and

others, 2022). Orthophosphate, TDP, TP, and DOC were positively correlated ($p<0.01$) with surface air temperature. These positive correlations with temperature could be explained by increases in microbial decomposition with increasing temperature (Kirschbaum, 2010) that increase the supply of these nutrients that are available for transport (Freeman and others, 2001; von Lützow and Kögel-Knabner, 2009). NO_3 plus NO_2 ($p<0.01$) and NH_4 and SiO_2 concentrations ($p<0.05$) were negatively correlated with surface air temperature. These negative correlations with temperature could be explained by increased uptake by algae in the aquatic environment under higher temperature conditions (Reay and others, 1999; Singh and Singh, 2015).

NO_3 plus NO_2 and SiO_2 ($p<0.01$) and NH_4 and TN ($p<0.05$) concentrations were positively correlated with runoff and may be explained by the same processes described above for precipitation. Orthophosphate and TDP were negatively correlated ($p<0.01$) with runoff. Mechanistic explanations for these negative correlations are not known. Orthophosphate, TDP, TP, and DOC concentrations were positively correlated ($p<0.01$) with downwelling shortwave radiation. Mechanistic explanations for these positive correlations are not known. NO_3 plus NO_2 ($p<0.01$) and NH_4 and SiO_2 ($p<0.05$) concentrations were negatively correlated with downwelling shortwave radiation. These negative correlations with radiation could be explained by increased uptake by algae in the aquatic environment due to higher rates of photosynthesis under conditions of higher solar radiation (Singh and Singh, 2015).

NO_3 plus NO_2 ($p<0.01$), NH_4 ($p<0.1$), and SiO_2 ($p<0.1$) concentrations were negatively correlated with ocean water temperature. Higher ocean water temperatures on the flood tides may be associated with increased algal growth and uptake of NO_3 plus NO_2, NH_4 and SiO_2, resulting in the observed negative correlations (Reay and others, 1999; Singh and Singh, 2015). Orthophosphate, TDP, and DOC ($p<0.01$) and TP ($p<0.05$) concentrations were positively correlated with ocean water temperature. Mechanistic explanations for these positive correlations and ocean water temperature are not known.

There was a substantial amount of missing data for atmospheric deposition of NO_3 plus NO_2 plus NH_4; however, using the existing data, there was a weak positive correlation ($p<0.1$) between atmospheric deposition of NO_3 plus NO_2 plus NH_4 and for NO_3 plus NO_2 concentrations on the ebb tide but no significant correlations for NH_4 or TN. Nutrient concentrations on the ebb tide were not correlated with mean sea level in Woods Hole.

The concentrations of NO_3 plus NO_2, NH_4, TN, TDP, and SiO_2 measured in surface water in Wellfleet Harbor during May through October were not significantly correlated with concentrations of those nutrients on the ebb tide at the Herring River during those months. The concentrations of orthophosphate and TP in surface water in Wellfleet Harbor were weakly positively correlated ($p<0.1$) with concentrations of those nutrients on the ebb tide at the Herring River during those months.

Table 3. Kendall's rank correlation tests for monthly variables and concentrations on the ebb tide in the Herring River at Chequessett Neck Road in Wellfleet, Massachusetts.

[Sign and statistical significance of Kendall's rank correlation tests are listed. Monthly variables are environmental variables, and monthly concentrations are average nutrient and suspended sediment concentrations. NO_3, nitrate; NH_4, ammonium; +, positive correlation; −, negative correlation; ***, $p<0.01$; **, $p<0.05$; *, $p<0.1$; NS, not statistically significant; NA, not applicable]

Nutrient concentration, ebb tide	Precipitation	Air temperature	Runoff	Solar radiation	Ocean water temperature	Atmospheric deposition of NO_3 and NH_4	Mean sea level
NO_3	+ ***	− ***	+ ***	− ***	− ***	+ *	NS
NH_4	+ ***	− **	+ **	− **	− *	NS	NS
Total nitrogen	+ ***	NS	+ **	NS	NS	NS	NS
Orthophosphate	NS	+ ***	− ***	+ ***	+ ***	NA	NS
Total dissolved phosphorus	NS	+ ***	− ***	+ ***	+ ***	NA	NS
Total phosphorus	NS	+ ***	NS	+ ***	+ **	NA	NS
Silica	+ ***	− **	+ ***	− **	− **	NA	NS
Dissolved organic carbon	NS	+ ***	NS	+ ***	+ ***	NA	NS
Suspended sediment concentration	NS	NS	NS	NS	NS	NA	NS

Summary

Nutrient concentrations across the ocean-estuary boundary of the Herring River in Wellfleet, Massachusetts, were assessed by the U.S. Geological Survey, in cooperation with the National Park Service and Friends of Herring River, from November 2020 to December 2021 to augment previous studies of baseline chemical characteristics. The purpose of these studies was to quantify the natural variability in nutrient and other constituent concentrations prior to future removal and re-engineering of a dike that has restricted saltwater inputs into the watershed for more than 100 years. Resource managers at the Cape Cod National Seashore would be able to use this information in adaptive management planning in the phased reintroduction of saltwater into the Herring River watershed.

This study also used the long-term U.S. Geological Survey dataset at this site from previous studies in conjunction with the data from this study to relate the observed variation in nutrient concentrations to season of the year and monthly average precipitation, temperature, runoff, solar radiation, ocean water temperature, mean sea level, atmospheric deposition of inorganic nitrogen, and inorganic nitrogen concentrations in Wellfleet Harbor. In addition, this study compared nutrient concentrations on flood versus ebb tide and spring, neap and midamplitude flood and ebb tides.

In this study, samples were collected at fixed times after the beginning of flood and ebb tides. Constituent concentrations generally were lower using this fixed time sampling than in previous studies that used flow-weighted composite sampling except for nitrate plus nitrite and orthophosphate. Concentrations of nitrate plus nitrite, ammonium, total nitrogen, total dissolved nitrogen, silica, and dissolved organic nitrogen generally were higher on the ebb tide than on the flood tide. By contrast, concentrations of orthophosphate, total phosphorus, and total dissolved phosphorus were generally similar between flood and ebb tides.

There was seasonal variation in most nutrient concentrations except silica and ammonia on flood and ebb tides. For phosphorus species, total nitrogen, and dissolved organic carbon, concentrations generally peaked in mid- to late summer and were lowest in winter. For nitrate, the reverse was true. There were minor differences for some constituents between spring, neap, and midamplitude tides for flood and ebb tides. Monthly average nitrate plus nitrite, ammonium, total nitrogen, and silica concentrations were positively correlated with precipitation and runoff. Orthophosphate, total dissolved phosphorus, total phosphorus, and dissolved organic carbon concentrations were positively correlated with surface air temperature, downwelling shortwave radiation, and ocean water temperature.

References Cited

Abatzoglou, J.T., 2013, Development of gridded surface meteorological data for ecological applications and modelling: International Journal of Climatology, v. 33, no. 1, p. 121–131. [Also available at https://doi.org/10.1002/joc.3413.]

ASTM International, 1999, Standard test methods for determining sediment concentration in water samples: ASTM International Standard D3977–97(2019), 7 p. [Also available at https://www.astm.org/d3977-97r19.html.]

Ballard, T.C., Sinha, E., and Michalak, A.M., 2019, Long-term changes in precipitation and temperature have already impacted nitrogen loading: Environmental Science & Technology, v. 53, no. 9, p. 5080–5090. [Also available at https://doi.org/10.1021/acs.est.8b06898.]

Bogen, J., 2004, Erosion and sediment yield in the Atna River basin: Hydrobiologia, v. 521, nos. 1–3, p. 35–47. [Also available at https://doi.org/10.1023/B:HYDR.0000026349.91866.94.]

Carlson, C.S., Masterson, J.P., Walter, D.A., and Barbaro, J.R., 2017a, Development of simulated groundwater-contributing areas to selected streams, ponds, coastal water bodies, and production wells in the Plymouth-Carver region and Cape Cod, Massachusetts: U.S. Geological Survey Data Series 1074, 17 p., accessed June 23, 2022, at https://doi.org/10.3133/ds1074.

Carlson, C.S., Masterson, J.P., Walter, D.A., and Barbaro, J.R., 2017b, Simulated groundwater-contributing areas to selected streams, ponds, coastal water bodies, and production wells, Plymouth-Carver region and Cape Cod, Massachusetts: U.S. Geological Survey data release, accessed June 23, 2022, at https://doi.org/10.5066/F7V69H2Z.

Center for Coastal Studies, 2022, Water quality monitoring program: Center for Coastal Studies web page, accessed July 14, 2022, at https://coastalstudies.org/cape-cod-bay-monitoring-program/. [Station data directly accessed at http://www.capecodbay-monitor.org/stations/43.]

Chaffee, C., Ferguson, W., and Ekberg, M.C., 2012, Salt marsh restoration in Rhode Island, *in* Roman, C.T., and Burdick, D.M., eds., Tidal marsh restoration—A synthesis of science and management: Washington, D.C., Island Press, p. 157–164.

Climatology Lab, 2017, gridMET—1 Jan–9 Nov 2017 ET0 (mm): Climatology Lab dataset, accessed July 18, 2021, at https://www.climatologylab.org/gridmet.html.

Freeman, C., Evans, C.D., Monteith, D.T., Reynolds, B., and Fenner, N., 2001, Export of organic carbon from peat soils: Nature, v. 412, no. 6849, p. 785–785. [Also available at https://doi.org/10.1038/35090628.]

Garrett, C., 1972, Tidal resonance in the Bay of Fundy and Gulf of Maine: Nature, v. 238, no. 5365, p. 441–443. [Also available at https://doi.org/10.1038/238441a0.]

Guy, H.P., 1969, Laboratory theory and methods for sediment analysis: U.S. Geological Survey Techniques of Water-Resources Investigations, book 5, chap. C1, 58 p. [Also available at https://doi.org/10.3133/twri05C1.]

Huntington, T.G., 2023, Data supporting analysis of relations between nutrient concentrations in the Herring River on the ebb tide, near Wellfleet, Massachusetts, and environmental conditions, 2015–2022: U.S. Geological Survey data release, https://doi.org/10.5066/P9ZU5YHW.

Huntington, T.G., and Spaetzel, A.B., 2020, Tidal daily discharge and quality assurance data supporting an assessment of water quality and discharge in the Herring River, Wellfleet, Massachusetts, November 2015–September 2017: U.S. Geological Survey data release, accessed June 23, 2022, at https://doi.org/10.5066/P9BKW4BX.

Huntington, T.G., Spaetzel, A.B., Colman, J.A., Kroeger, K.D., and Bradley, R., 2021, Assessment of water quality and discharge in the Herring River, Wellfleet, Massachusetts, November 2015 to September 2017: U.S. Geological Survey Scientific Investigations Report 2020–5120, 59 p., accessed June 23, 2022, at https://doi.org/10.3133/sir20205120.

Kirschbaum, M.U.F., 2010, The temperature dependence of organic matter decomposition—Seasonal temperature variations turn a sharp short-term temperature response into a more moderate annually averaged response: Global Change Biology, v. 16, no. 7, p. 2117–2129. [Also available at https://doi.org/10.1111/j.1365-2486.2009.02093.x.]

LeBlanc, D.R., Guswa, J.H., Frimpter, M.H., and Londquist, C.J., 1986, Ground-water resources of Cape Cod, Massachusetts: U.S. Geological Survey Hydrologic Atlas 692, 4 pls. [Also available at https://doi.org/10.3133/ha692.]

Masterson, J.P., 2004, Simulated interaction between freshwater and saltwater and effects of ground-water pumping and sea-level change, lower Cape Cod aquifer system, Massachusetts: U.S. Geological Survey Scientific Investigations Report 2004–5014, 72 p. [Also available at https://doi.org/10.3133/sir20045014.]

McCabe, G.J., and Markstrom, S.L., 2007, A monthly water-balance model driven by a graphical user interface: U.S. Geological Survey Open-File Report 2007–1088, 6 p. [Also available at https://doi.org/10.3133/ofr20071088.]

National Atmospheric Deposition Program, 2018, Site NTN MA01: National Atmospheric Deposition Program data, accessed November 26, 2018, at https://nadp.slh.wisc.edu/sites/ntn-ma01/. [Annual precipitation data retrieved.]

National Oceanic and Atmospheric Administration [NOAA], 2022a, Relative sea level trend—8447930 Woods Hole, Massachusetts: National Oceanic and Atmospheric Administration Tides & Currents data, accessed July 14, 2021, at https://tidesandcurrents.noaa.gov/sltrends/sltrends_station.shtml?id=8447930.

National Oceanic and Atmospheric Administration [NOAA], 2022b, Station 44013 (LLNR 420)—Boston 16 NM East of Boston, MA: National Oceanic and Atmospheric Administration National Data Buoy Center data, accessed July 14, 2022, at https://www.ndbc.noaa.gov/station_page.php?station=44013.

National Oceanic and Atmospheric Administration [NOAA], 2022c, Station 44090—Cape Cod Bay, MA (221): National Oceanic and Atmospheric Administration National Data Buoy Center data, accessed July 14, 2022, at https://www.ndbc.noaa.gov/station_page.php?station=44090.

National Park Service, Town of Wellfleet, Mass., Town of Truro, and Herring River Restoration Committee, 2016, Herring River restoration project—Final environmental impact statement/environmental impact report, May 2016: National Park Service, 446 p., accessed October 6, 2017, at https://parkplanning.nps.gov/document.cfm?parkID=217&projectID=18573&documentID=73471.

Patton, C.J., and Kryskalla, J.R., 2003, Methods of analysis by the U.S. Geological Survey National Water Quality Laboratory—Evaluation of alkaline persulfate digestion as an alternative to Kjeldahl digestion for determination of total and dissolved nitrogen and phosphorus in water: U.S. Geological Survey Water-Resources Investigations 03–4174, 33 p. [Also available at https://doi.org/10.3133/wri034174.]

Portnoy, J.W., 1999, Salt marsh diking and restoration—Biogeochemical implications of altered wetland hydrology: Environmental Management, v. 24, no. 1, p. 111–120. [Also available at https://doi.org/10.1007/s002679900219.]

Portnoy, J.W., and Allen, J.R., 2006, Effects of tidal restrictions and potential benefits of tidal restoration on fecal coliform and shellfish-water quality: Journal of Shellfish Research, v. 25, no. 2, p. 609–617. [Also available at https://doi.org/10.2983/0730-8000(2006)25[609:EOTRAP]2.0.CO;2.]

Portnoy, J.W., and Giblin, A.E., 1997a, Biogeochemical effects of seawater restoration to diked salt marshes: Ecological Applications, v. 7, no. 3, p. 1054–1063. [Also available at https://doi.org/10.1890/1051-0761(1997)007[1054:BEOSRT]2.0.CO;2.]

Portnoy, J.W., and Giblin, A.E., 1997b, Effects of historic tidal restrictions on salt marsh sediment chemistry: Biogeochemistry, v. 36, no. 3, p. 275–303. [Also available at https://doi.org/10.1023/A:1005715520988.]

Reay, D.S., Nedwell, D.B., Priddle, J., and Ellis-Evans, J.C., 1999, Temperature dependence of inorganic nitrogen uptake—Reduced affinity for nitrate at suboptimal temperatures in both algae and bacteria: Applied and Environmental Microbiology, v. 65, no. 6, p. 2577–2584. [Also available at https://doi.org/10.1128/AEM.65.6.2577-2584.1999.]

Roman, C.T., 1987, An evaluation of alternatives for estuarine restoration management—The Herring River ecosystem (Cape Cod National Seashore): National Park Service Cooperative Research Unit, Rutgers University, 200 p. [Also available at https://archive.org/details/evaluationofalte00roma/page/n1/mode/2up.]

Roman, C.T., and Burdick, D.M., 2012, Tidal marsh restoration—A synthesis of science and management: Washington, D.C., Island Press, 432 p.

Singh, S.P., and Singh, P., 2015, Effect of temperature and light on the growth of algae species—A review: Renewable and Sustainable Energy Reviews, v. 50, p. 431–444. [Also available at https://doi.org/10.1016/j.rser.2015.05.024.]

Smith, S.M., 2007, Removal of salt-killed vegetation during tidal restoration of a New England salt marsh: effects on wrack movement and the establishment of native halophytes: Ecological Restoration, v. 25, no. 4, p. 268–273. [Also available at https://doi.org/ 10.3368/er.25.4.268.]

Sommer Mess Systemtechnik, 2014, RG–30, RG–30a—Velocity measurement system—User manual: Sommer Mess Systemtechnik, 62 p., accessed February 6, 2019, at https://www.hydroscientificwest.com/cms/docs/Manual%20RG-30%20SW-ver%201_5x%20%20ENG%202012-Jan.pdf.

Sorenson, J.R., Granato, G.E., and Smith, K.P., 2018, Nutrient and metal loads estimated by using discrete, automated, and continuous water-quality monitoring techniques for the Blackstone River at the Massachusetts-Rhode Island State line, water years 2013–14: U.S. Geological Survey Scientific Investigations Report 2017–5094, 41 p., accessed January 30, 2023, at https://doi.org/10.3133/sir20175094.

Soukup, M.A., and Portnoy, J.W., 1986, Impacts from mosquito control-induced sulphur mobilization in a Cape Cod estuary: Environmental Conservation, v. 13, no. 1, p. 47–50. [Also available at https://doi.org/10.1017/S0376892900035864.]

Sugimura, Y., and Suzuki, Y., 1988, A high-temperature catalytic oxidation method for the determination of non-volatile dissolved organic carbon in seawater by direct injection of a liquid sample: Marine Chemistry, v. 24, no. 2, p. 105–131. [Also available at https://doi.org/10.1016/0304-4203(88)90043-6.]

Teledyne ISCO, 2015, 6712 Portable samplers installation and operation guide: Teledyne Inc., 242 p. [Also available at https://www.uvm.edu/bwrl/lab_docs/manuals/ISCO_6712_autosampler.pdf.]

Town of Wellfleet, 2019, Herring River adaptive management plan, attachment 8.B *of* Herring River restoration project—Development of regional application impact application: Town of Wellfleet, 32 p. accessed February 3, 2023, at https://www.capecodcommission.org/resource-library/file?url=%2Fdept%2Fcommission%2Fteam%2Fmember%2FProject+Documents%2FInactive+Reviews%2FDRIs%2FHerring+River+Restoration+Plan%2FLtd+DRI+application+December+2019%2F2019-12-12-Herring+River++Restoration+Project-DRI+Application.pdf. [Attachment contents available at https://www.capecodcommission.org/resource-library/file?url=%2Fdept%2Fcommission%2Fteam%2Fmember%2FProject+Documents%2FInactive+Reviews%2FDRIs%2FHerring+River+Restoration+Plan%2FLtd+DRI+application+December+2019%2FSection+8+attachments+A-G%2FAttachments+As+Individual+Files%2FSection+8.B_HRAMP_11Dec2019.pdf.]

U.S. Environmental Protection Agency, 1993, Method 350.1—Determination of ammonia nitrogen by semi-automated colorimetry (revision 2.0): U.S. Environmental Protection Agency, 15 p. [Also available at https://www.epa.gov/esam/epa-method-3501-determination-ammonia-nitrogen-semi-automated-colorimetry.]

U.S. Geological Survey, 2015, StreamStats: U.S. Geological Survey web page, accessed July 19, 2018, at http://www.usgs.gov/streamstats.

U.S. Geological Survey, 2022, USGS water data for the nation: U.S. Geological Survey National Water Information System database, accessed July 15, 2022, at https://doi.org/10.5066/F7P55KJN.

U.S. Geological Survey, [variously dated], National field manual for the collection of water-quality data: U.S. Geological Survey Techniques of Water-Resources Investigations, book 9, chaps. A1–A10, [variously paged], accessed July 18, 2017, at https://doi.org/10.3133/twri09.

von Lützow, M., and Kögel-Knabner, I., 2009, Temperature sensitivity of soil organic matter decomposition—What do we know?: Biology and Fertility of Soils, v. 46, no. 1, p. 1–15. [Also available at https://doi.org/10.1007/s00374-009-0413-8.]

Warren, R.S., Fell, P.E., Rozsa, R., Brawley, A.H., Orsted, A.C., Olson, E.T., Swamy, V., and Niering, W.A., 2002, Salt marsh restoration in Connecticut—20 years of science and management: Restoration Ecology, v. 10, no. 3, p. 497–513. [Also available at https://doi.org/10.1046/j.1526-100X.2002.01031.x.]

Western Regional Climate Center, 2018, Weather data for the Wellfleet, Massachusetts, monitoring site: Western Regional Climate Center climate data, accessed April 12, 2018, at https://raws.dri.edu/cgi-bin/rawMAIN.pl?ncMCAP.

Winter, C., Tarasova, L., Lutz, S.R., Musolff, A., Kumar, R., and Fleckenstein, J.H., 2022, Explaining the variability in high-frequency nitrate export patterns using long-term hydrological event classification: Water Resources Research, v. 58, no. 1, paper e2021WR030938, 21 p., accessed March 30, 2023, at https://doi.org/10.1002/essoar.10507676.1.

Zhang, J.-Z., and Berberian, G.A., 1997, Method 366—Determination of dissolved silicate in estuarine and coastal waters by gas segmented continuous flow colorimetric analysis: U.S. Environmental Protection Agency EPA/600/R–15/010, 13 p. [Also available at https://cfpub.epa.gov/si/si_public_record_report.cfm?Lab=NERL&dirEntryId=309419.]

Zhang, J.-Z., Ortner, P. B., and Fischer, C. J., 1997, Method 353.4—Determination of nitrate and nitrite in estuarine and coastal waters by gas segmented continuous flow colorimetric analysis [revision 2.0]: U.S. Environmental Protection Agency EPA/600/R–15/012, 20 p. [Also available at https://cfpub.epa.gov/si/si_public_record_report.cfm?Lab=NERL&dirEntryId=309421.]

Zimmerman, C.F., and Keefe, C.W., 1997, Method 365.5—Determination of orthophosphate in estuarine and coastal waters by automated colorimetric analysis [revision 1.4]: U.S. Environmental Protection Agency EPA/600/R–15/011, 9 p. [Also available at https://cfpub.epa.gov/si/si_public_record_Report.cfm?Lab=NERL&dirEntryId=309420.]

Appendix 1. Monthly Average Concentrations of Contaminants and Climatic Conditions on the Herring River at Near Wellfleet, Massachusetts

This appendix includes monthly average concentrations of contaminants and climatic conditions on the ebb tide on the Herring River at Chequessett Neck Road, near Wellfleet, Massachusetts from June 2016 to December 2017 and June 2020 to December 2021.

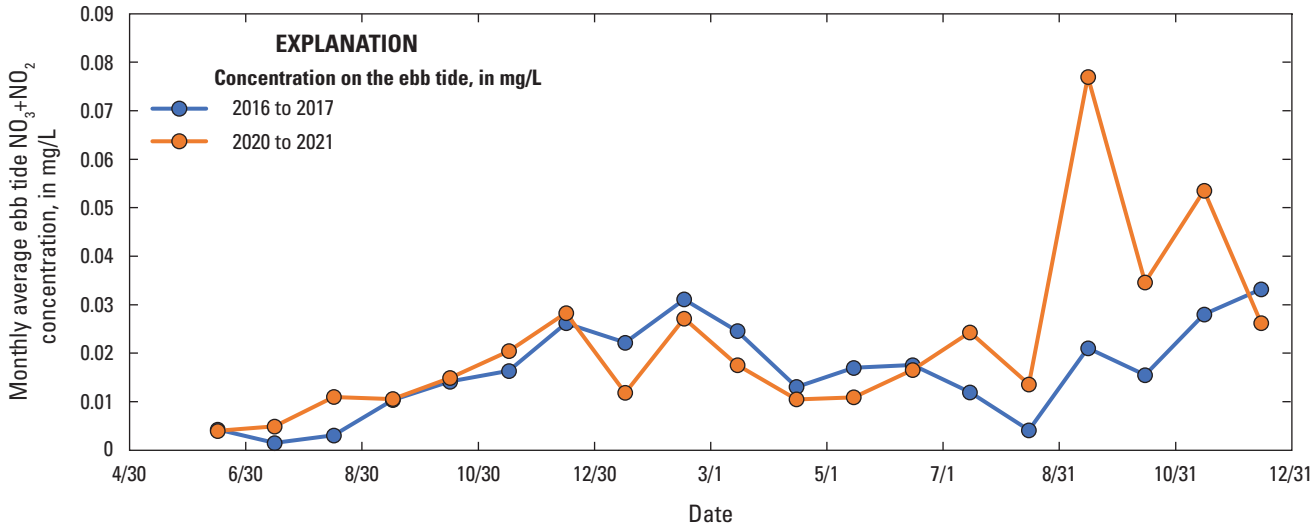

Figure 1.1. Graph showing monthly average nitrate (NO_3) and nitrite (NO_2) concentration over time for the early (June 2016 to December 2017) and recent periods (June 2020 to December 2021) in the Herring River at Chequessett Neck Road, Near Wellfleet, Massachusetts. $NO_3 + NO_2$, nitrate plus nitrite; mg/L, milligram per liter.

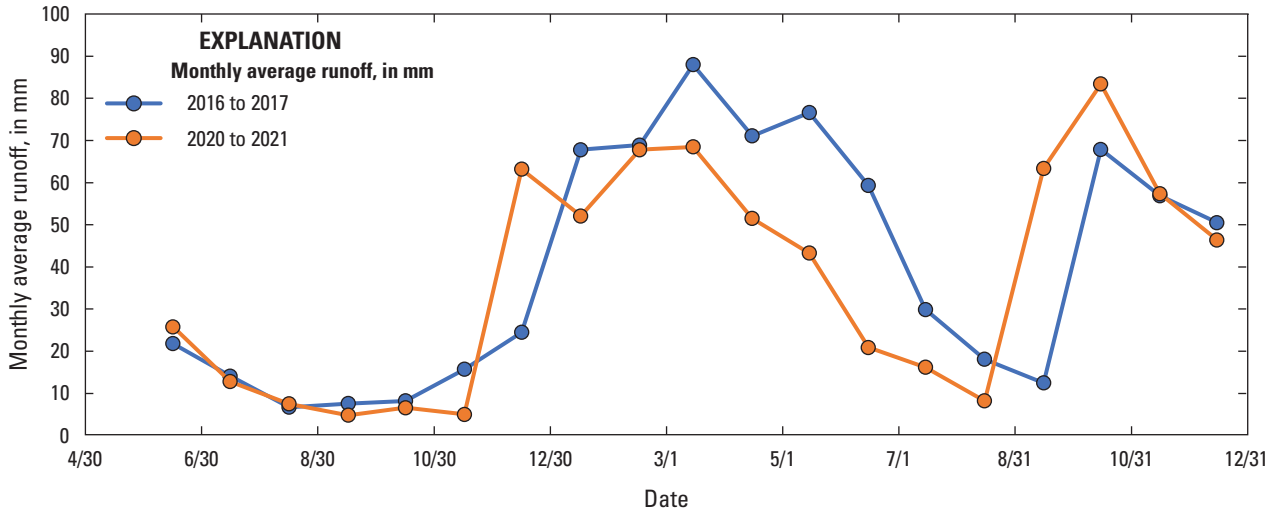

Figure 1.2. Monthly average runoff versus time for the early (June 2016 to December 2017) and recent periods (June 2020 to December 2021) in the Herring River at Chequessett Neck Road, Near Wellfleet, Massachusetts. mm, millimeter.

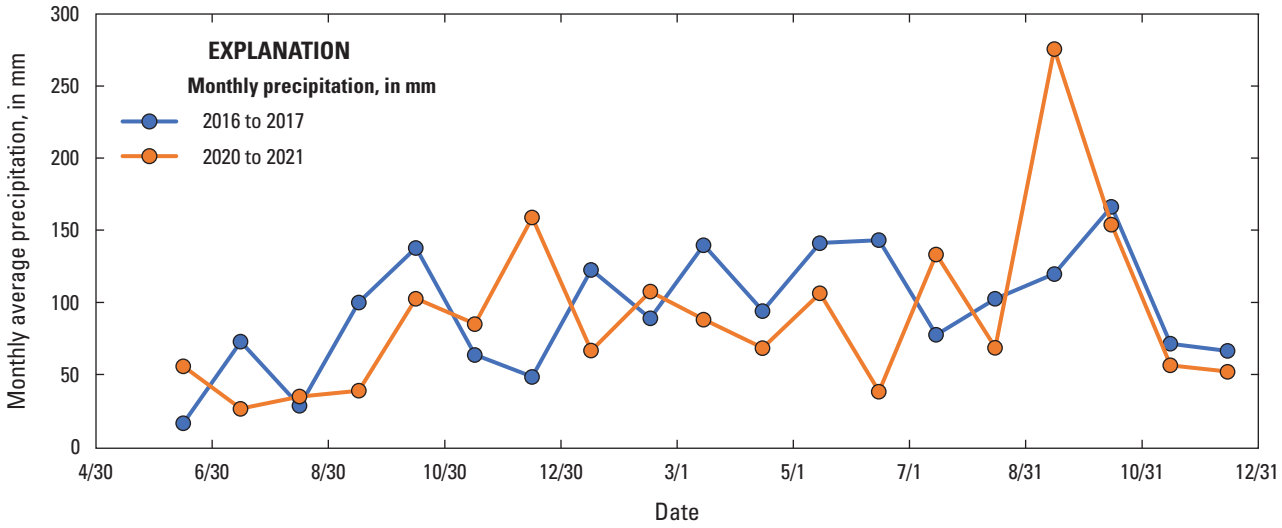

Figure 1.3. Monthly average precipitation versus time for the early (June 2016 to December 2017) and recent periods (June 2020 to December 2021) in the Herring River at Chequessett Neck Road, Near Wellfleet, Massachusetts. mm, millimeter.

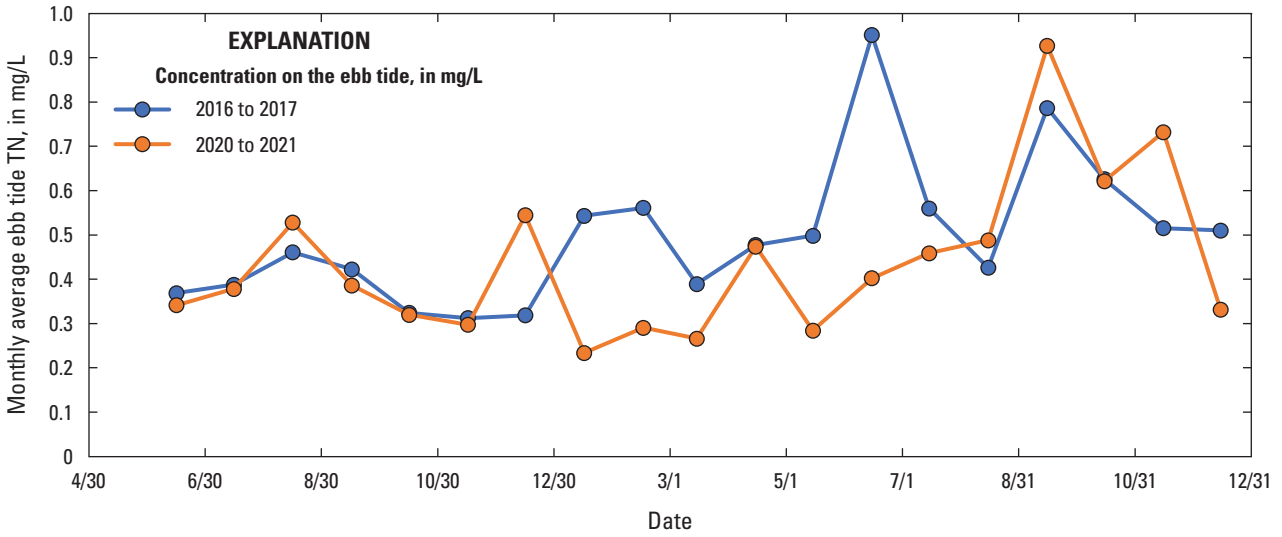

Figure 1.4. Monthly average total nitrogen concentration versus time for the early (June 2016 to December 2017) and recent periods (June 2020 to December 2021) in the Herring River at Chequessett Neck Road, Near Wellfleet, Massachusetts. TN, total nitrogen; mg/L, milligram per liter.

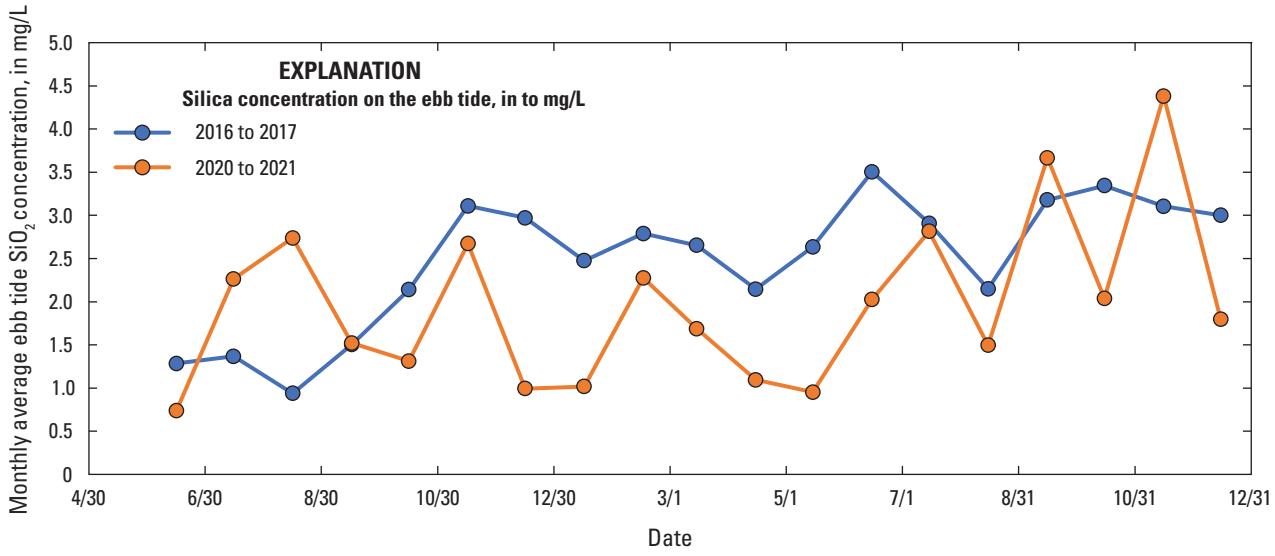

Figure 1.5. Monthly average silica concentration versus time for the early (June 2016 to December 2017) and recent periods (June 2020 to December 2021) in the Herring River at Chequessett Neck Road, Near Wellfleet, Massachusetts. SiO_2, silica; mg/L, milligram per liter.

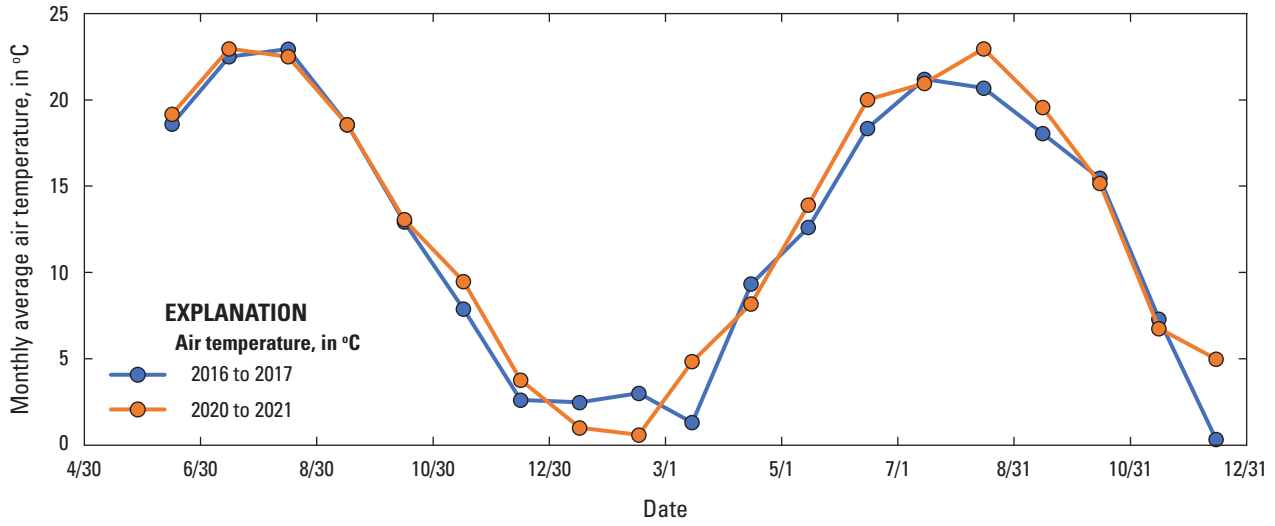

Figure 1.6. Monthly average air temperature versus time for the early (June 2016 to December 2017) and recent periods (June 2020 to December 2021) in the Herring River at Chequessett Neck Road, Near Wellfleet, Massachusetts. °C, degree Celsius.

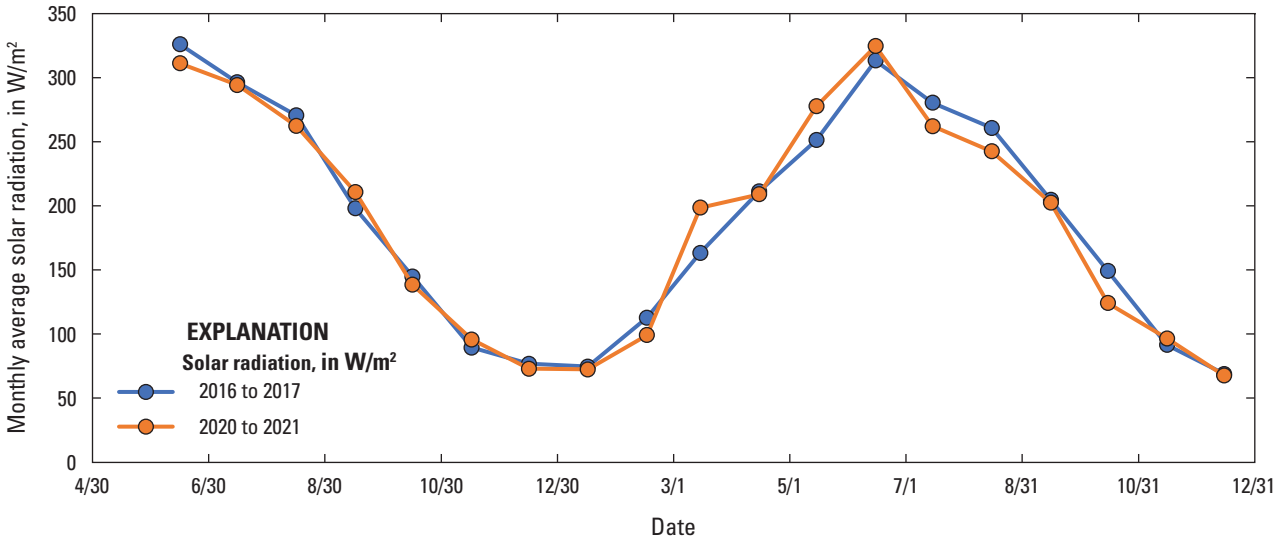

Figure 1.7. Monthly average solar radiation versus time for the early (June 2016 to December 2017) and recent periods (June 2020 to December 2021) in the Herring River at Chequessett Neck Road, Near Wellfleet, Massachusetts. W/m², watt per square meter.

Appendix 2. Field Methods—Interim Announcement for Change in Capsule-Filter Type, Supplier, and Instructions for Use

Available as a portable document format (PDF) file at https://doi.org/10.3133/sir20235120.

Appendix 3. Alert and Preliminary Guidance for Addressing Nitrogen Contamination of Pall Versapor GWV High-Capacity Capsule Filters

Available as a portable document format (PDF) file at https://doi.org/10.3133/sir20235120.

For more information, contact
Director, New England Water Science Center
U.S. Geological Survey
10 Bearfoot Road
Northborough, MA 01532
dc_nweng@usgs.gov
or visit our website at
https://www.usgs.gov/centers/new-england-water

Publishing support provided by the
Pembroke Publishing Service Center

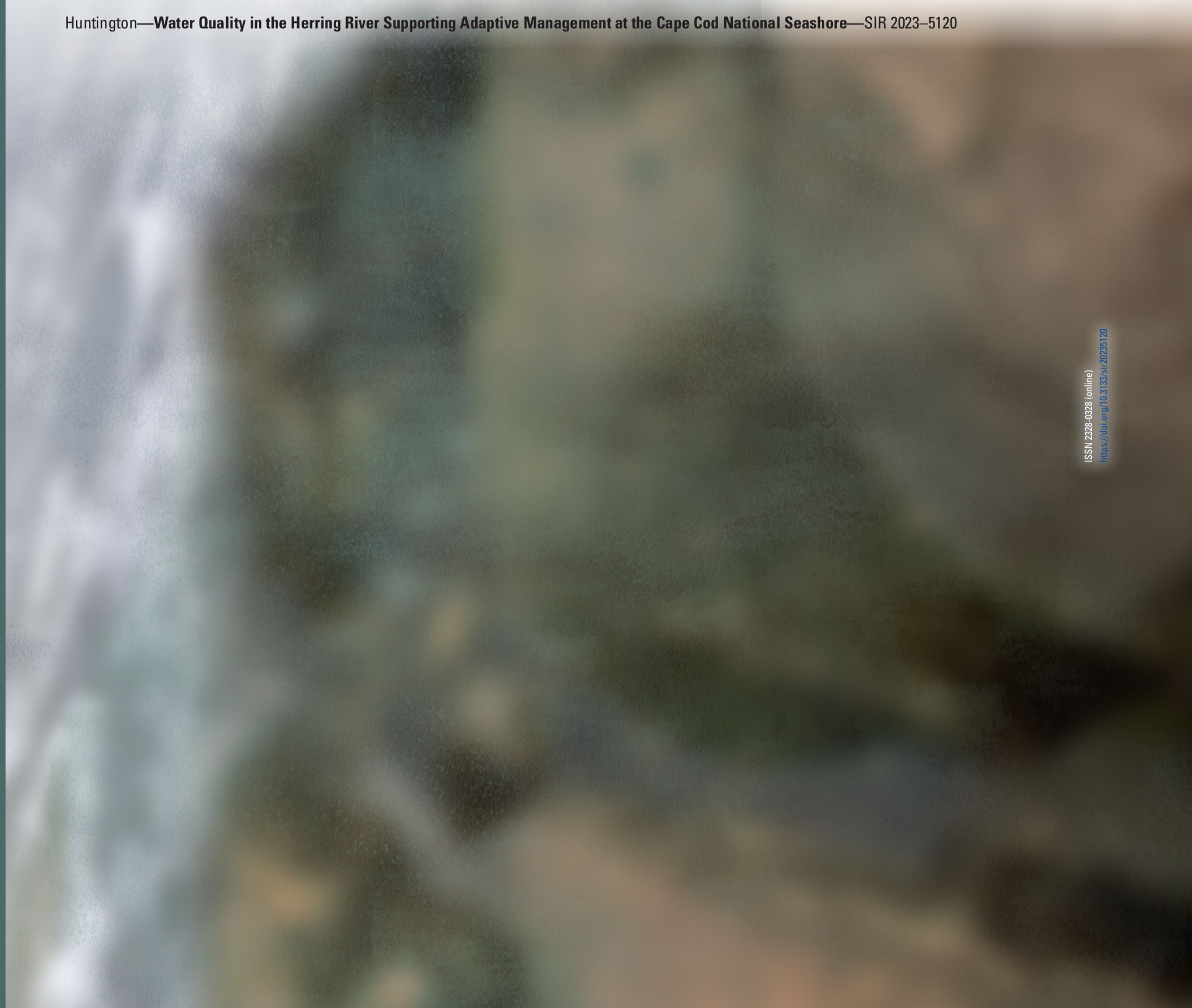

ISSN 2328-0328 (online)
https://doi.org/10.3133/sir20235120